View metadata, citation and similar papers at core.ac.uk

brought to you by CORE

provided by Marshall University

Marshall University
Marshall Digital Scholar

Theses, Dissertations and Capstones

2013

Toward a Comprehensive Model of Photosystem II Oxygen Evolving Complex Photoassembly

James Scott Board II
Board13@marshall.edu

Follow this and additional works at: http://mds.marshall.edu/etd

 Part of the Biochemistry Commons, Chemistry Commons, and the Plant Sciences Commons

Recommended Citation

Board, James Scott II, "Toward a Comprehensive Model of Photosystem II Oxygen Evolving Complex Photoassembly" (2013). *Theses, Dissertations and Capstones.* Paper 475.

This Thesis is brought to you for free and open access by Marshall Digital Scholar. It has been accepted for inclusion in Theses, Dissertations and Capstones by an authorized administrator of Marshall Digital Scholar. For more information, please contact zhangj@marshall.edu.

TOWARD A COMPREHENSIVE MODEL OF PHOTOSYSTEM II OXYGEN EVOLVING COMPLEX PHOTOASSEMBLY

Thesis submitted to
the Graduate College of
Marshall University

In partial fulfillment of the
requirements for the degree of
Master of Science

in

Chemistry

by
James Scott Board II

Approved by

Dr. Derrick R. J. Kolling, Committee Chairperson
Dr. Leslie Frost
Dr. Bin Wang

Marshall University

May 2013

Acknowledgments

I would first like to thank my wonderful and loving wife Erica Board who has supported me in everything I have done. She has been a there for me always, from checking the grammar in my paper to providing the moral support I need when I am frustrated and just want to give up, I couldn't do it without her. I would also like to thank my parents James and Melissa Board who have always supported me and told me I can be anything I wanted as long as I worked hard and applied myself. Most of my family hasn't pursued any kind of advanced education and it was only because of the support of my family that I have been able to not only to earn a bachelor's degree but now a master's degree in chemistry as well.

I would like to thank my advisor, Dr. Derrick Kolling. You have helped to guide and educate me these last few years and I have learned so much from you. You have taught me valuable skills in the lab and in life. I cannot thank you enough for all that you have done for me while I was here at Marshall. I would like to thank all of members of the Kolling lab, both past and present. From Ben Blodgett who helped train me when I came to the lab, Anthony Stephenson who performed the manganese assay for me, and Matt Thompson who was always good company on the many hours we spent taking measurements in the darkroom.

I would like to thank my committee members Dr. Leslie Frost and Dr. Bin Wang for your guidance and support in writing my thesis. I would also like to add a special thanks to Dr. Frost for helping me do the silver stain to my gel and for helping me get an image of the gel after we had stained it. I would like to thank Dr. Bob Morgan and Caleb Calvary who have been such good friends during my time in the graduate program; they have listened to me complain when experiments were not going my way and always made me feel better about it. I would like to thank the Marshall University Chemistry Department. Without which I would not have been able to accomplish all the things that I have.

Table of Contents

List of Figures

at a concentration of 12.5 µg/ml [Chl *a*] and an illumination intensity of 750 µE from prep 1 (12/11/11).

Figure 14. A comparison of the temperature dependence titration for OEC depleted (apo-BBYs) (blue line) and intact BBY particles (red line). Apo-BBYs were made using a pH 9.5 CHES buffer and reassembly of the cluster was done using 200 µl $CaCl_2$ (stock 10 mM), 100 µL of $K_3[Fe(CN)_6]$ (stock 50 mM), 50 µL of $MnCl_2$ (stock 2 mM), 50 µL of sodium bicarbonate (stock 20 mM), 5 µL of apo-BBY (stock 2.5 mg/mL), and 595 µL of K3, with a final volume of 1 mL. Actinic pulsed light at a rate of 100 per min for 10 min experiments were conducted using BBYs with a concentration of 12.5 µg/ml [Chl *a*] and an illumination intensity of 750 µE prep 1 (12/11/11).

Figure 15. Percent recovery of oxygen evolution rates for the apo-BBY particles. Experiments were conducted using BBYs with a concentration of 2.5 mg/mL [Chl *a*] (stock) and a working concentration of 5 µg/ml using prep 1 (12/11/11). Photoassembly was conducted as described in Figure 13.

Figure 16. Percent recovery of oxygen evolution rates for the apo-BBY particles when treated with protease inhibitor cocktail. Experiments were conducted using BBYs with a concentration of 12.5 µg/ml [Chl *a*] and an illumination intensity of 750 µE using prep 1 (12/11/11). Photoassembly was conducted as described in Figure 13.

Figure 17. Degradation experiments in which BBYs were incubated that 28 °C (red bar) and then at 35 °C for the specified times with measurements of oxygen evolution.

Figure 18. A $[K_3Fe(CN)_6]$ titration at the temperature maxima of 28°C. Experiments were conducted using BBYs with a concentration of 12.5 µg/ml [Chl *a*] and an illumination intensity of 750 µE using prep 1 (12/11/11). Photoassembly was conducted as described in Figure 11 and in the presence of protease inhibitor cocktail.

Figure 19. A flash titration of the photoassembly of apo-BBYs oxygen evolution rates with 1 mM $K_3[Fe(CN)_6]$ using photoassembly procedures described in Fig. 13. The titration was performed at 5 °C (blue diamond), 10 °C (red square), 15 °C (green triangle), 20 °C (purple X), 25 °C (blue *), and 35 °C (orange circle). Experiments were conducted using apo-BBYs with a concentration of 12.5 µg/ml [Chl *a*] and an illumination intensity of 750 µE using prep 2 (5/14/12) in the presence of protease inhibitor cocktail.

Figure 20. Flash titration of oxygen evolution rates at 1 mM (blue diamonds), 5 mM (red squares), and 10 mM (green triangles) $[K_3Fe(CN)_6]$. Experiments were conducted using apo-BBYs with a concentration of 12.5 µg/ml [Chl *a*] and an illumination intensity of 750 µE using prep 2 (5/14/12). Photoassembly was conducted as described in Figure 13 and in the presence of protease inhibitor cocktail.

Figure 21. A 5 °C flash titration of oxygen evolution rates at 1 mM (blue diamonds), 5 mM (red squares), 10 mM (green triangles), and 15 mM (purple plus signs) [$K_3Fe(CN)_6$]. Experiments were conducted using apo-BBYs with a concentration of 12.5 µg/ml [Chl *a*] and an illumination intensity of 750 µE using prep 3 (10/13/12). Photoassembly was conducted as described in Figure 13 and in the presence of protease inhibitor cocktail.

Figure 22. 40 °C flash titration of oxygen evolution rates at 1 mM (blue diamond), 5 mM (red square), and 10 mM (green triangle) [$K_3Fe(CN)_6$]. Experiments were conducted using apo-BBYs with a concentration of 12.5 µg/ml [Chl *a*] and an illumination intensity of 750 µE using prep 3 (10/13/12). Photoassembly was conducted as described in Figure 13 and in the presence of protease inhibitor cocktail.

Figure 23. A flash frequency titration of oxygen evolution rates under different $K_3Fe(CN)_6$ concentrations. [$K_3Fe(CN)_6$] at 0.5 mM (blue diamond), 1 mM (red square), and 5 mM (green triangle). Experiments were conducted using BBYs with a concentration of 12.5 µg/ml [Chl *a*] and an illumination intensity of 750 µE using prep 2 (5/14/12). Photoassembly was conducted as described in Figure 13 and in the presence of protease inhibitor cocktail.

Figure 24. A flash frequency titration of photoassembly oxygen evolution rates using $K_3Fe(CN)_6$ 5 mM at 28 °C(blue diamond), 5 °C (red square), and 40 °C (green triangle). Experiments were conducted using BBYs with a concentration of 12.5 µg/ml [Chl *a*] and an illumination intensity of 750 µE using prep 2 (5/14/12). Photoassembly was conducted as described in Figure 13 and in the presence of protease inhibitor cocktail.

Figure 25. Effect of [$K_3Fe(CN)_6$] on rates of apo-BBY oxygen evolution. The concentrations tested were 0.5 mM (purple dashes), 1 mM (blue diamonds), 2.5 mM (red squares), and 5 mM (green triangles). Experiments were conducted using BBYs with a concentration of 12.5 µg/ml [Chl *a*] and an illumination intensity of 750 µE using prep 2 (5/14/12). Photoassembly was conducted as described in Figure 13 and in the presence of protease inhibitor cocktail.

Figure 26. Flash titration at 5mM [$K_3Fe(CN)_6$] for oxygen evolution of intact BBY particles 28°C (blue diamonds), 5°C (red square), and 40°C (green triangle). Experiments were conducted using BBYs with a concentration of 12.5 µg/ml [Chl *a*] and an illumination intensity of 750 µE from prep 2 (5/14/12) and in the presence of protease inhibitor cocktail.

Figure 27. A titration of the dark step of photoassembly using a 1 second pre flash. Experiments were conducted using BBYs with a concentration of 12.5 µg/ml [Chl *a*] and an illumination intensity of 750 µE using prep 3 (10/13/12) and in the presence of protease inhibitor cocktail.

Figure 28. Newly proposed model for photoassembly that incorporates both traditional models as well and the data relating to the inactivation under highlight conditions.

Abstract

Elucidating the mechanism of photoassembly of the oxygen-evolving complex (OEC) will lead to a better understanding of how nature catalyzes water oxidation. Although the temperature dependence of oxygen evolution has been described in the literature *[1,2]*, we have performed a comprehensive study that covers Photosystem II (PSII) activity oxygen evolution in the presence and absence of 2,6-dichloro-1,4benzoquinone (DCBQ) from 5–45°C. In addition, we performed similar measurements for OEC photoassembly in the absence of DCBQ. PSII-enriched particles used for our measurements were prepared according to Berthold, Babcock, and Yocum *[3]*, with modifications from Kolling, *et al*.*[4]* The oxygen-evolution of intact BBY particles at a temperature range of 5–45°C was measured and found to have a maximum at 28°C, which is consistent with literature values[4]. We then generated OEC-depleted BBY (apo-BBY) particles by using an established aminosulfonic buffer (20 mM CHES/NaOH, pH 9.4) and a divalent cation (200 mM $MgCl_2$) treatment with minor modifications. *[1]* These apo-BBY particles were combined with a mixture of Mn^{2+}, Ca^{2+}, HCO^{3-}, and $K_3[Fe(CN)_6]$ and then subjected to light pulses within a temperature range of 5–45 °C followed by oxygen-evolution measurements at 28°C. The apo-BBYs were then subjected to different $K_3[Fe(CN)_6]$ concentrations and a range of pulses with varying flash number and frequency in order probe the rate limiting step of photoassembly. The shared temperature profiles between oxygen evolution and photoassembly, as well as the frequency titrations and $K_3[Fe(CN)_6]$ concentration experiments, have contributed to a more comprehensive model of photoassembly of the PSII protein complex. Experiments with DCBQ during PSII water oxidation were found to flatten the temperature-dependence profile in the range of 10–32°C; and protease activity within the BBY preps also showed a temperature dependence and was responsible for some loss of activity over 28°C. These new data will lead to a better understanding of how PSII functions.

1. Introduction

Photosynthetic systems are regularly used for development and application of new and advancing technologies, such as specially tailored molecules with reaction centers that mimic that of PSII, with applications for solar fuels and solar cells and genetically engineered higher order plants.

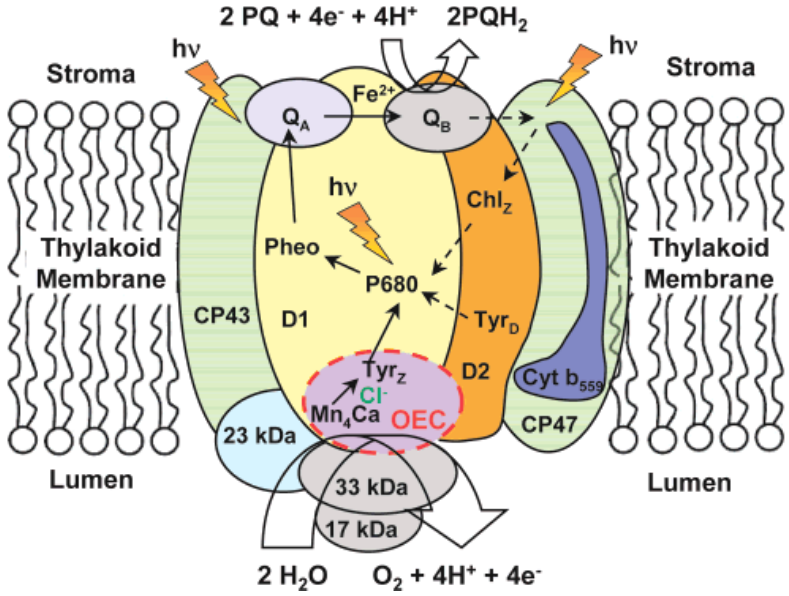

Figure 1. A cartoon of the Photosystem II protein within the thylakoid membrane of a chloroplast. The PSII protein complex includes its subunits, the electron transfer pathway occurring within the protein, and the splitting of water occurring at the OEC.

Why is the study of photosynthetic processes important? Although the photosynthetic systems are considered to be well characterized, the mechanisms that are at work within the PSII protein complex need further elucidating. Kinetic, as well as pH experiments, will deepen our understanding of these mechanisms. Photosynthetic study is important to enzyme kinetics research because of the difficulty of measuring the kinetics of a typical enzyme reaction in the desired time scale of ms due to the lengthy time requirements of combining the substrates and

enzymes. With photosynthesis, the reaction can be driven by pulses of light and the reaction can be measured on the scale of 1ps to several ms by the use of laser spectroscopy and optical spectroscopy. Another important feature of photosynthesis is the reaction center; it is, in essence, an assembly of cofactors that are held in a suitable position by the protein environment (Figure 1). Using this model, several research groups have designed organic molecules with different cofactors and have created "artificial reaction centers." These include cofactors such as manganese oxides and cobalt-borate and cobalt oxides *[5,6]*. These molecules can be introduced into liposomes, and, when they are excited by light, the charge separation will create an electric potential. The electric potential may serve in a variety of purposes including the synthesis of ATP. Further study of photosynthesis has led to genetic modifications of proteins and higher plants. Genetic modification has lead to other advances in the modification of higher plants as well. The original direction for genetic modification of higher plants was to increase the efficiency of photosynthesis; however, this genetic modification has not been successful so modification of PSII is being investigated as a potential way of increasing photosynthetic efficiency *[7]*. The focus has shifted in other labs to the production of compounds that engage in "artificial photosynthesis." Artificial photosynthesis is the splitting of water and the production of hydrogen PSII at a separate site. Oxygen is produced in the PSII protein complex at the manganese cluster also known as the OEC. This type of research into the study of how the manganese cluster, the catalyst for water oxidation, is photoassembled has led to the development of many chemicals. Chemicals such as blue dimer that mimic photosynthetic water splitting can be used in photochemical solar cells with a possible application in the production of organic fuel cells *[8]*. Although the blue dimer molecule was not very efficient, it was the first step in developing molecules that would mimic the reaction centers in PSII by performing

photoassembly and splitting water. Now cobalt oxide nanocrystals are being used to accomplish this process. They are efficient, fast, very abundant, and will last a long time *[9,10,11]*. The idea of the artificial leaf, a solar cell that can mimic natural water oxidation to generate electricity, has been around for over a decade. Daniel Nocera has worked to develop the next generation in artificial leaf technology by creating a solar cell that mimics photosynthesis using a cobalt oxide in order to split water into hydrogen and oxygen, which are stored in a fuel cell and used for electricity. It is reported that this cell is 4.7 percent efficient at photosynthesis and can run for 45 hours continuously without a drop in activity. Although this solar cell may not be an immediate end to energy needs, it is the first critical step in the right direction. This solar cell is not the first artificial leaf, but it is the first practical one. The first leaf was developed over a decade ago and used strong acid base reactions and rare and expensive materials. This new leaf has been developed using abundant low cost earth metals, and it works at a near neutral pH. This cell can even be paired with a fuel forming catalyst to generate direct "solar-to-fuel" pathways that will allow the H_2 and O_2 to be used in fuel cells *[5]*.

The photoinhibition mechanism is another unresolved question in the photosynthetic community. Photoinhibition is the process by which light actually damages and reduces the efficiency of photosynthetic mechanism *[12]*. The exact mechanism for this inhibition is not clear, and there are several proposed models that require testing in order to validate or exclude. These models include (1) acceptor-side photoinhibition, in which strong light reduces the plastoquinone pool and leads to nonfunctional Q_a and to inhibited PSII *[13]*, (2) donor-side photo-inhibition, in which some PSII centers are not active and are extremely sensitive to light and become permanently inhibited *[14,15]*, (3) manganese mechanism, a photon is absorbed by the manganese ions of the OEC which triggers inactivation of the oxygen-evolving complex

[16], (4) singlet oxygen inhibition, in which singlet oxygen is formed by weakly coupled chlorophylls or by cytochromes and this oxygen damages the cluster *[17,18]*, and (5) low light inhibition in which low light conditions allow for charge recombination forming triplet P_{680} which harms the cluster *[19]*. By unraveling the mysteries of photoinhibition, scientists could find a way to circumvent photoinhibition to increase the yields in crops, biofuels production, or even increase the efficiency of the artificial leaf.

Photosynthesis is the biological process by which the Sun's energy is converted, through a series of steps, into biochemical energy to be used by plants, some algae, and some bacteria. This process has proven to be essential to all life and, over the past 450 million years, has created a world with an oxygen-rich atmosphere. Photosynthesis literally is "synthesis with light." One may think this concept means that any process involving synthesis using light is photosynthesis. However, such is not the case because it would then include processes that are best left to be discussed separately. So, instead, one could say that "photosynthesis is a process in which light energy is captured and stored by an organism, and the stored energy is used to drive cellular processes *[8]*." Chlorophyll-based photosynthesis, which is the most common type of photosynthesis, operates using electron transfer processes and is present in plants and algae. The type of photosynthesis that takes place can be anoxygenic (non-oxygen producing) or oxygenic (oxygen producing) with chlorophyll-based being the latter. There is also bacterial rhodopsin-based photosynthesis, but it is mechanically very different from chlorophyll-based photosynthesis *[7,8,11,20]*. The main focus within the paper will be on the chlorophyll-type pigments found in plants and, to lesser extent, algae. The location of the chlorophyll pigments is a very important factor in photosynthesis research. The pigments are located in the chloroplasts,

the subcellular structure where all of the chlorophyll is located. In most organisms, the chloroplast is where all of the phases of the photosynthetic processes are carried out.

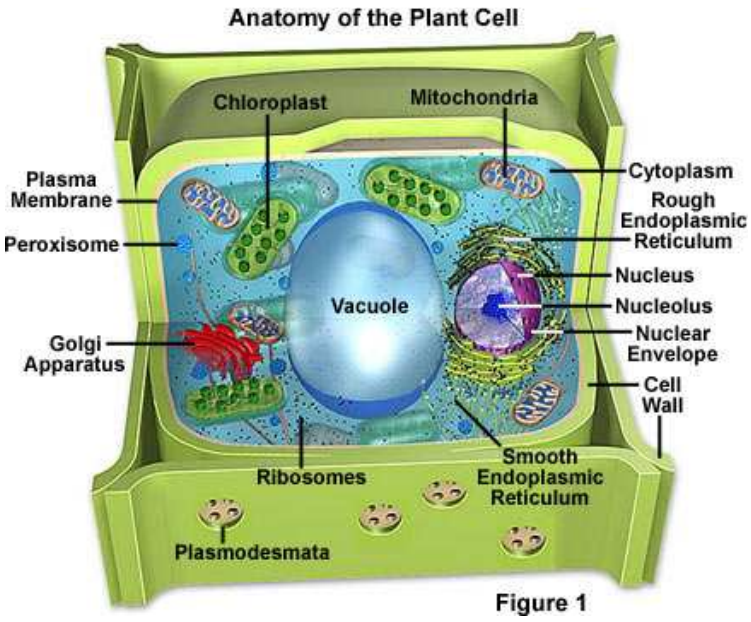

Figure 2. A plant cell including all of its organelles *[21]*.

In Figure 2, the chloroplasts can be seen in the cytoplasm and are about the size of bacteria, only a few μm in length, and even resemble a bacterium. The chloroplasts are in fact the result of symbiotic bacteria that integrated with the early plants and lost their autonomy over time.

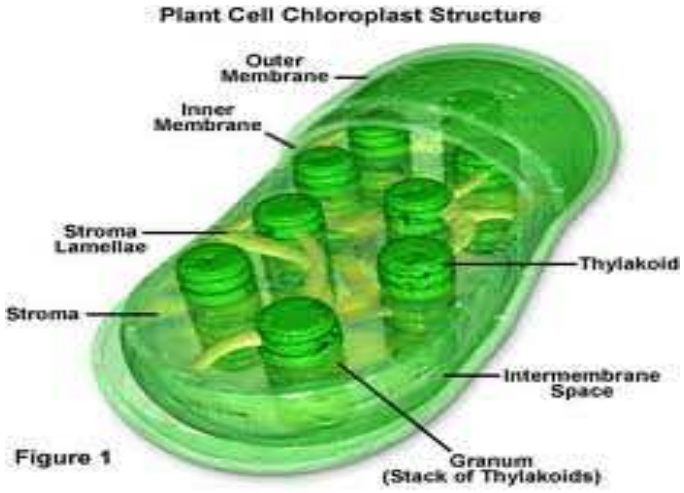

Figure 3. The interior of a chloroplast organelle *[22]*.

In Figure 3, the interior of the chloroplast can be seen including a membrane system known as the granum. These membranes can exist as closely stacked, or grana thylakoid membranes or as non stacked, or stroma thylakoid membranes. The aqueous phase found inside of the chloroplast is known as the stroma. The stroma contains soluble enzymes, functions as the site of carbon metabolism reactions, and is responsible for the products that are exported throughout the plant to support other cellular processes. There are roughly four phases that occur within the cell involving the production and transportation of energy in photosynthesis: (1) the light is absorbed and the energy is delivered by antenna systems, (2) primary electron transfer in the reaction centers occurs, (3) energy stabilization by a secondary process, and (4) the synthesis and export of stable products *[8]*. Within the thylakoid membrane, there exists a multiprotein complex PSII, which is involved in the first chemical process of photosynthesis. This assembly of proteins, usually more than 20 subunits, is responsible for water splitting and oxygen production in plants and algae. A major area of research is the mechanism for water splitting by PSII. To study this mechanism, one can use chlorophyll concentration and oxygen production to

get information about catalytic rate. In algae, the preparation can be accomplished with whole cells. However, this approach does not work in higher plants and the Berthold, Babcock, and Yocum preparation or BBY preparation is required. BBY particles are PSII-enriched membrane preparations *[23]*. The necessary type of particle is a high yield, highly active, and sufficiently pure PSII particle in order to do spectroscopic work and photoassembly research. With the implementation of partial detergent solubilization in the BBY protocol, PSII particle yield is extremely high in comparison to PSII core complex preparations and relatively stable in comparison to preparation of whole thylakoids. This preparation takes advantage of the grana thylakoids that are PSII rich. Grana stacking is more pronounced in plants, weaker in algae, and almost nonexistent in cyanobacteria, the latter having stroma thylakoids instead of grana. Due to BBY particles being better suited for various types of investigations than the core complex preparation particles, there is urgent need of protocols that will yield not only high quality but high amounts of PSII particles *[23]*.

In order to begin research into photoassembly, oxygen evolution, and fluorescence, a standard BBY preparation had to be established in the lab by modifying the existing protocol for changes in instrumentation, chemicals, and methods. Part of my project was this establishment of the protocol in the lab. I was able to accomplish the establishing of the protocol by completing several BBY preparations and making necessary changes for using spinach as a model organism. In addition, our values needed to be compared to the established literature values for concentration of chlorophyll *a* and oxygen evolution rates. Once the preparation was established and high-quality values were obtained for the BBY particles extracted from spinach, both temperature dependence and pH dependence experiments were able to be conducted to obtain a

better understanding of the mechanism and conformational changes occurring within the PSII protein complex during photoassembly.

Study of the temperature dependence of the intact BBY particle and the oxygen evolving cluster (OEC) yields a better understanding of the rate limiting step and the mechanism for photoassembly. In order to study the OEC in more detail and to understand the mechanisms involved, a way is needed to study just the OEC. In depth study of the OEC was accomplished by removing the extrinsic proteins: 23kDa, 33kDa, and the 17kDa and the OEC itself by the treatment of BBYs with a high pH buffer, followed by isolation of these depleted or apo-BBY particles (Figure 1). Metal salts can be added to apo-BBY particles, and when exposed to pulses of actinic light the OEC will reassemble minus the extrinsic proteins.

The model in Figure 1 indicates the path of electrons within the PSII protein complex. However, this model of the OEC fails to account for any potential rates of reaction, so it is still unknown where the rate limiting step is within this scheme. By comparing the temperature dependence of the intact PSII with the apo-BBYs, potential bottlenecks in the electron transport pathway of PSII can be better understood by studying the differences that occur in the processes.

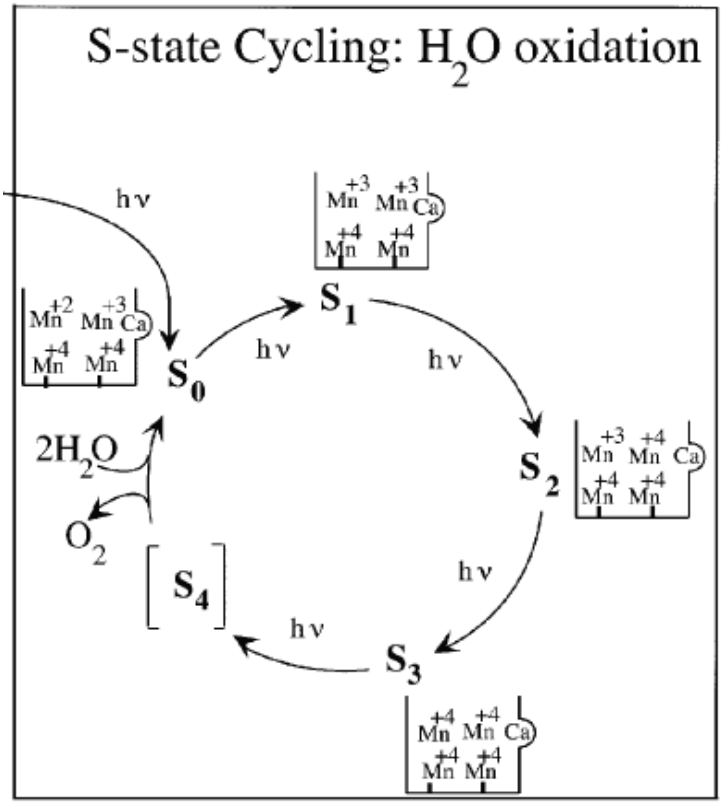

Figure 4. S-state cycle of the OEC and the charges carried by the Mn the in cluster *[25]*.

The charges that are currently believed to be carried by the manganese ions in the OEC can be seen in Figure 4 *[25]*. These are known as the high oxidation state model with S_0 having 2 Mn^{+4}s, a Mn^{+3}, and a Mn^{+2}. This high oxidation state model can be seen in Figure 4; however, there have been some new EPR data presented that show that the charges could in fact be lower than previously believed. These charges would be 3 Mn^{+3} and a Mn^{+2} for S_0 *[26,27]*.

When studying the pH dependence of photoassembly, potential ligand binding can be explored by titrating the pH of the ionizable groups for both the intact PSII and the apo-BBY. The pK_a can be calculated and then compared to already known pK_a values for amino acids believed to be involved in ligating to the OEC. This comparison of pK_a values of the amino acids

believed to be involved in ligand binding to the OEC with the experimentally determined pK_a values were the first steps to obtaining a clear picture of this binding. A better understanding of the process of photoassembly would make identifying the ligands from the pH experiments much simpler. Although it is known on a large scale where the electrons are going, the amino acids that are facilitating the electron transfer in close proximity to the OEC have not been definitively labeled *[7,8,25]*. This more complete understanding of all the processes involved in oxygen evolution will allow for the better creation of a higher efficiency biomimetic solar cell.

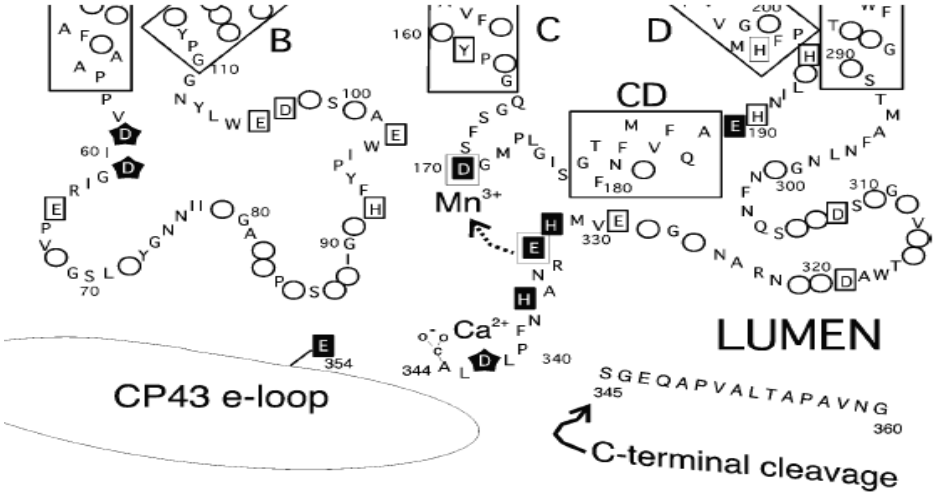

Figure 5. Amino acid diagram of the luminal area of the D1 subunit of photosystem II with potential Mn ligands in black rectangles and potential Ca^{2+} ligands as black pentagons *[25]*.

Figure 5 shows many of the potential ligands that have already been identified. The pH dependence studies of the PSII will provide a much needed basis for exploring which of these amino acids could be responsible for ligating to the OEC. Further spectroscopic analysis will be necessary, such as studying mutants that have the amino acids knocked out to see how these knockouts affects the formation of the cluster.

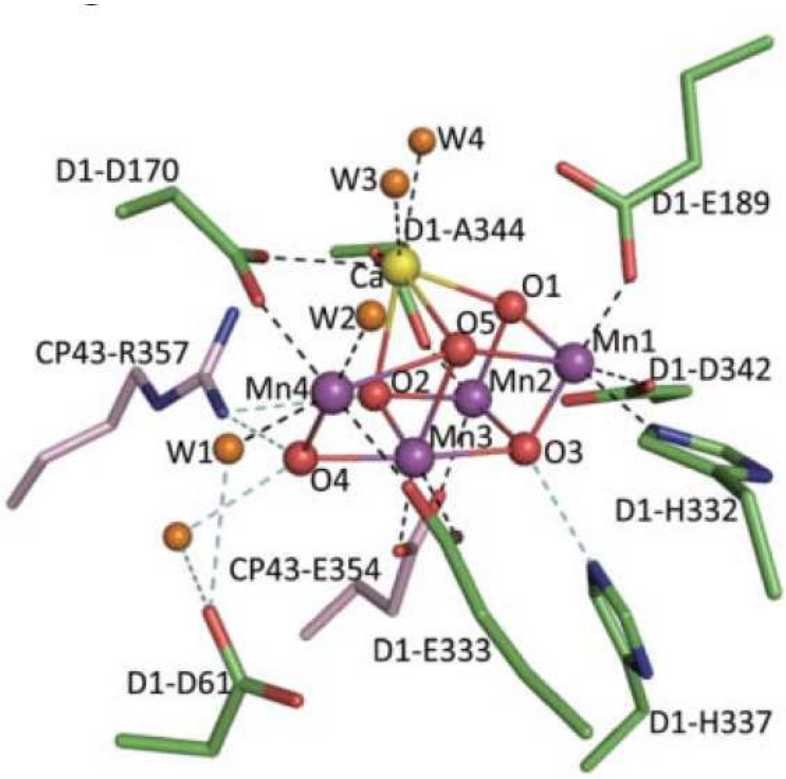

Figure 6. The most current proposal for the OEC and its potential ligands *[26]*.

Although Figure 6 does show some proposed ligands for the OEC, these have not been proven to actually ligate to the cluster as is shown above. With each new proposed structure, there are new suggested binding sites for the ligands within the D1 subunit. By conducting these pH dependence studies, a clearer picture of the actual ligating amino acids of the D1 subunit can be obtained. Once the ligands for the OEC have been identified, one more piece to the puzzle that is the OEC will be filled in and a more comprehensive understanding of the OEC and its photoassembly will be obtained.

By studying both the temperature and pH-dependence of the PSII protein of the higher order plant spinach, both the physical and chemical questions that have plagued this area of research can finally begin to be answered. To date, the rate limiting step and the ligand binding sites have not been determined by traditional methods due to the sensitive nature of this protein. Obtaining a better understanding of this protein, which is essential to both the flora and fauna of the word, will contribute to better methods for mimicking and harnessing this protein. The benefits could come in the form of something as life changing as a natural solar cell that would be cleaner and more renewable than the silica versions of today. It could even come in the form of a modified PSII protein complex that would allow for better growth of plants in climates that were previously inhospitable to plants, allowing for increased world crop production.

By looking at pulsed versus continuous light and its effect on photoassembly, a better understanding of photoassembly and photoinhibition can be obtained. Current experiments are normally performed using pulsed light which makes it difficult to determine kinetic data from these experiments. Micro constants, constants that explain one discrete step, can be harder to obtain using pulsed light due to their short lived nature in the OEC. A continuous light source will make the kinetic information much easier to obtain, and this alternate type of experiment will allow for the elucidation of a more complete mechanism of photoassembly (Figure 7). In addition, understanding photoassembly will further understanding of the photoinhibition since

photoassembly is so critical to the reset of photoinhibition.

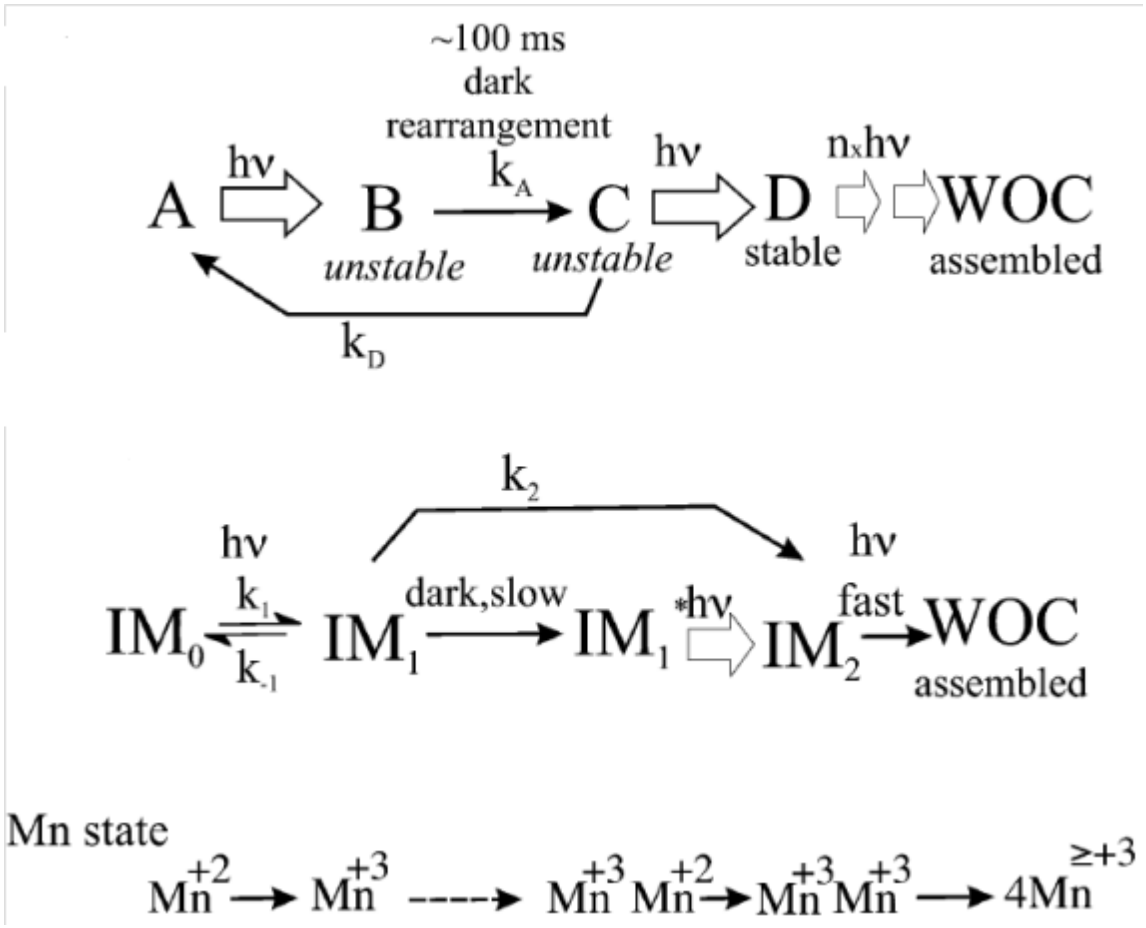

Figure 7. A comparison of the schemes of the two basic quantum mechanisms for photoassembly proposed by Cheniae and by Zaltsman et al. *[25]*.

Figure 7 is the current proposed mechanism for photoassembly that was first put forth by Cheniae and then Zaltsman et al [25,33,35]. The Cheniae scheme shows the stability of each intermediate as well as a reverse reaction that will take the cluster back to its first stage and allow for reformation. In the Zaltsman model showed in Figure 7, the reversible reaction going from IM_0 to IM_1 can be seen with there being a slow dark step to get to IM_1^*. From IM_1^* there needs to be another photon of light to progress the partially formed cluster to IM_2 and then a third photon

to get to the fully assembled OEC, according to the low oxidation state model. These are both incomplete models and require further elaboration in order to fully explain the mechanism by which the OEC is assembled into a functional cluster that can oxidize water. Through frequency experiments, as well as the study of the effect of $K_3[Fe(CN)_6]$ on photoassembly, a better understanding of photoassembly and photoinhibition will be obtained. By understanding photoinhibition, the process can be controlled in order to increase oxygen evolution.

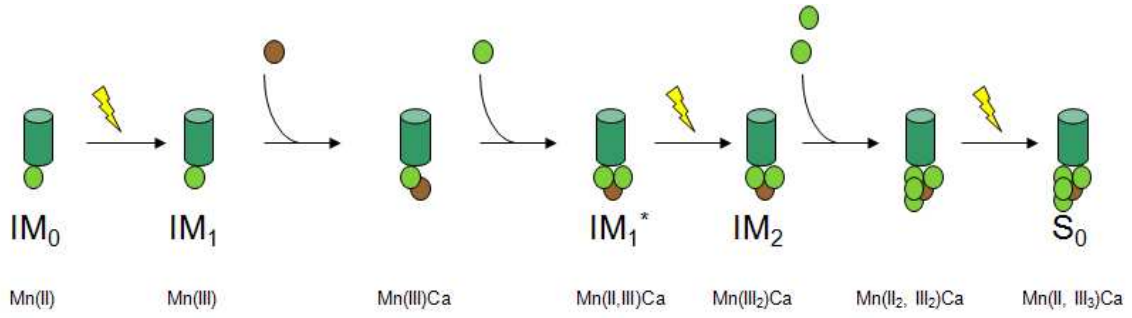

Figure 8. The model of photoassembly and how it relates to PSII.

Figure 8 helps to understand the models presented in Figure 7 by illustrating how the Ca and Mn are integrated into PSII in each of the intermediate steps all leading up to the complete S_o that starts the S-state cycle. It can be seen that in IM_0 and IM_1 a single Mn goes from Mn^{+2} to Mn^{+3}. The Ca and another Mn^{+2} are added to the cluster to generate the IM_1^*. The light driven increase in charge of the second Mn from Mn^{+2} to Mn^{+3} creates IM_2. The incorporation of the final two Mn^{+2} generates a completed OEC.

2. Materials and Methods

2.1 BBY Preparation for Spinach

To begin the BBY preparation, the first item that had to be obtained was fresh spinach. Spinach was used as it is high in chlorophyll and was traditionally used to isolate PSII. Baby leaf spinach was used initially, due to an inability to obtain fresh fully grown spinach, and was mainly used to test the changes to the procedure and to make corrections. In the next preparation, curly leaf spinach was utilized. Then two final preparations were done with the desired adult flat leaf spinach. The freshest possible whole spinach plants were needed due to the fact that, once picked, the proteases begin to cause the plant proteins to deteriorate. Once the plants were obtained, the petioles, or the center vein in the plant, had to be removed due to the large concentration of proteases that it contains. Gloves where worn during the BBY preparation in order to protect the mixture from proteases that are present on the skin. After approximately 2 L of leaves had their petioles removed, the leaf pieces were processed through a Super Angel juicer to begin the extraction of the BBY particles. The leaves were juiced in a Super Angel triturating juicer which sped up the preparation due to its ability to strain the pulp using a fine holed strainer system and lyse the cells into a solution of K1 grinding buffer. This K1 solution contained 0.1 M sucrose 0.2 M NaCl, 35 mM HEPES and protease inhibitor cocktail (Calbiochem). The protease inhibitor cocktail contained 5 different protease inhibitors: 4-(2-Aminoethyl) benzenesulfonyl fluoride hydrochloride (AEBSF) and bovine lung which inhibit serine proteases, aprotinin which is a broad spectrum inhibitor, and E-64, leupeptin hemisulfate inhibits which work on cysteine and trypsin like proteases to help inhibit the enzymes that cause protein degradation. The different buffers were used to provide a stable pH environment for the plant cells and later the

membranes as the desired products were obtained. The juicing of the spinach produced approximately 500 mL of a lysate and buffer solution. It was then strained and put into five 100 mL centrifuge tubes and centrifuged at 4˚C and at 3000 Xg for 2min in a Beckman Coulter Allegra 64 R centrifuge. This low speed, short spin removed some of the undesirable material from the solution; the supernate was decanted into five more 100mL centrifuge tubes and spun at 4˚C and 8600Xg for 15 min. This resulted in a pellet containing the desired material. The pellets were dissolved in a minimal amount of K2 buffer (0.4 M sucrose, 5 mM NaCl, 5 mM $MgCl_2$•$6H_2O$, 15 mM $CaCl_2$ (AN), 50 mM MES•H_2O) and were mixed together and homogenized so that a concentration of chlorophyll could be obtained at this point. The concentration of chl *a* was determined using a Shimadzu UV-1800 scanning UV-Vis and the equation:

$$[\text{Chl } a] \text{ (mg/mL)} = ((OD_{652} - OD_{750}) \times \text{optical path length (cm)} \times 27.8 \times \text{D.F.} / 1000) \quad \text{(eq. 1)}$$

The amount of Triton X-100 was calculated for the following step based upon the chl *a* concentrations obtained. The suspension of thylakoid membranes K2 in buffer was placed in a beaker, and the beaker was placed into an ice bath. The suspension was slowly stirred with a magnetic stirrer and Triton X-100 (20% w/v) was slowly added along the walls of the beaker until the ratio of 20 mg Triton X-100: 1 mg Chl was obtained. The final [Chl *a*] was ~ 2 mg/mL. The solution was stirred for 12 min in the ice bath at 4 °C. The Triton X-100 began to break down the ends of the grana on the thylakoid membrane. It was previously reported that the Triton exposure time should not exceed 30 min due to the possibility of it deteriorating too much of the membrane *[3]*. After 12 min, the solution was transferred to four 25 mL centrifuge tubes and the tubes were spun at 4˚C and 40 000 Xg for 18 min. The supernate contained light-harvesting antenna and PSI. The pellet was then resuspended in K2 and protease inhibitor cocktail, and the

25 mL tubes are filled completely with K2. They were spun at 40 000 Xg for 18 min. at 4˚C, and the pellet was then resuspended in K3 buffer containing (50 mM MES, 35 mM NaCl, 0.3 M sucrose), which left the white starch portion of the pellet behind. The suspension was then transferred to four 25 mL centrifuge tubes and spun at 40 000 Xg for 18 min. at 4˚C. If the supernate was clear, it could be decanted and the pellets resuspended in a minimal amount of K3; however, if the supernate was not clear then it was decanted and the step was repeated until it was clear. After the BBY particles were suspended in a minimal amount of K3, the highly enriched PSII particles were then dropped into liquid nitrogen using a glass dropper. The pellets were then transferred into a 50-mL disposable conical vial and stored in liquid nitrogen for use in photoassembly and fluorescence tests.

2.2 Modifications to the BBY Preparation

The BBY preparation is usually done in a walk in cooler set to 4˚C to maintain the stability of the sample during the preparation. The first protocol change was to modify a Styrofoam box to use as an ice bath and add cold packs to the juicer and the Triton ice bath due to a lack of the walk in cooler. The use of a blender was changed to a triturating juicer which sped up the preparation, due to its ability to strain the pulp and lyse the cells. The amount of straining needed was reduced due to the juicer allowing for separation of the pulp, which the blender did not. The addition of the protease inhibitor cocktail was beneficial due to the fact that the individual protease inhibitors that the preparation had originally called for were highly unstable at room temperature and still barely usable at 4˚C. The protease inhibitor phenylmethanesulfonyl fluoride (PMSF) was only stable at room temperature for 30 min and ε-ACA while being stable for 3 months at 4˚C still had a diminished shelf life. The new dry cocktail came in a powder form and was mixed right before the preparation started. The mixture

remained viable for about 24 h, so two preparations could be done from one batch of cocktail. The preparation's size was also cut in half from a 1 L preparation to a 500 mL preparation due to the limitations of the centrifuge.

2.3 Oxygraph Measurement

After the BBY particles were frozen in liquid nitrogen, 1-2 pellets were thawed in an eppendorf tube that was placed in an ice bath. Once the pellets were thawed, 5 µL of sample was pipetted into an eppendorf tube and then diluted to 1 mL with 80% acetone, which was done twice to obtain an average. Afterward, the two samples were spun in an Eppendorf mini spin micro-centrifuge at 14 000 Xg, and the supernate was decanted into a quartz cuvette with a 1 mm path length. The absorbance at 652 nm and 750 nm were recorded and the final chl *a* concentration was calculated using equation 1. With a final average concentration calculated from the two samples. The working concentration could be calculated using:

$$M_1V_1 = M_2V_2 \text{ (eq. 2)}$$

since the sample was diluted to 5 µL per 1mL. The 5 µL of BBYs were added to an eppendorf tube, then 100 µL of potassium ferrocyanide ($K_3[Fe(CN)_6]$) was added and the total volume was brought to 1 mL with the addition of K3 buffer. The oxygen evolution measurements were all conducted with illumination being provided by the lowest amount of green light possible in order to ensure that the PSII complex was excited in the least amount possible. The reason for the green light was due to green light being the wavelength that is absorbed least by PSII. The 1 mL of sample was then added to the oxygraph, and the inlet tube was then capped to prevent the loss of oxygen that was produced from oxygen evolution. The oxygraph was then covered with a box to allow it to dark acclimate for 5 min. Measurements were recorded throughout this dark

acclimation. After 5 min, the light was turned on, and the cover was removed from the box. The slope of the line from the oxygen being produced was recorded and the calculation:

(μmol O_2/mg Chl *a*/h) = (slope x 60 / 1000) / working concentration (eq 3)

From this the amount of oxygen in μmol, produced per mg of chl *a* per hour was calculated.

2.4 Optimization of Testing Condition

After the different samples were tested for PSII activity the sample with the highest activity and largest quantity was selected to be used for the optimization of the oxygen evolving testing conditions. The first condition to be optimized was the concentration of $K_3Fe(CN)_6$ that was used. A titration of $K_3Fe(CN)_6$ was done from .5mM to 10mM. After this was accomplished, the concentration of DCBQ was optimized from 0μM to 300μM. The final condition that had to be optimized was the temperature at which the oxygen evolution tests would be performed. The temperature dependence curve was done between the temperatures of 5 °C through 40 °C.

2.5 Apo-BBY Preparation

In order to study photoassembly of the OEC, the OEC must first be removed along with the extrinsic proteins that surround it on the luminal side of the membrane. The removal of the extrinsic proteins and the OEC was accomplished by treatment with a 1ml CHES buffer which contains 35 mM NaCl, 300 mM sucrose, and 25mM N-cyclohexyl-2-aminoethanesulfonic acid (CHES). The 1ml CHES buffer, 200 μL 10mM $MgCl_2$, and 200 μL 2.5 mg/ml BBY solution was added to an eppendorf tube and mixed by inversion for 4 min. After this time it was added to 1.4 mL of K3, buffer and the reaction was quenched. At this point, the solution was in two eppendorfs which were spun in a micro centrifuge at 14 000 Xgs for 60 s. The supernatant was

then removed using a pipette, and the pellets were resolublized in 250 μL of K3 buffer each. They were then spun at 14,000 Xgs for 60 s, and this was repeated a total of three times after the initial spin in order to wash the pellets and remove the extrinsic proteins and the manganese and calcium from the BBYs. After the final spin the supernatant was removed and the pellets were combined by resolubliztion of both pellets using the same 200 μL of K3. The concentration of the apo-BBY was then checked and found to be 2.5 mg/mL.

2.6 Testing the Apo-BBYs for Activity and Performing Photoassembly

With the OEC depleted (apo-BBY) made, a test was performed to check for any remaining activity in the solution. This was done by the addition of 200 μl $CaCl_2$ (stock 10mM), 100 μL of $K_3[Fe(CN)_6]$ (stock 50mM), 5 μL of apo-BBY (stock 2.5 mg/mL), and 695 μL of K3 so the final vol. is 1 mL. The sample was then put into the oxygraph allowed to dark acclimate before being exposed to the projector lamp. No oxygen was produced from the sample indicating no intact OECs remained in the sample.

For photoassembly, a sample was prepared with 200 μl $CaCl_2$ (stock 10mM), 100 μL of $K_3[Fe(CN)_6]$ (stock 50 mM), 50 μL of $MnCl_2$ (stock 2 mM), 50 μL of sodium bicarbonate (stock 20mM), 5 μL of APO-BBY (stock 2.5 mg/mL), and 595 μL of K3 so the final vol. was 1 mL. The sample was then put into an incubator set to 28 °C and exposed to flashes of actinic light at a rate of 100 per minute for 10 min. The sample was then put into to oxygraph and after 5 minutes the oxygen evolution was measured.

2.7 Conformation of Removal of Extrinsic via SDS PAGE

Although the lack of oxygen evolution indicated that the OEC had been removed, this depletion of the OEC was confirmed by two different methods: an SDS PAGE to show the removal of the extrinsic proteins and a manganese assay to show complete removal of all the manganese.

SDS PAGE was accomplished by taking 50 µL aliquots of the intact BBYs, from each wash step, and from the apo-BBY sample. They were then mixed with 50µL of Bio-Rad's Laemmli sample buffer with dithothreitol (DTT) and heated at 95 °C for 10 min to denature the proteins. 10 µL of sample was then added to each lane of a precast 12- 20% gradient gel. The gel was then run at 200mV until the dye ran to the bottom of the gel, approximately 45 min. The gel was then stained with Coomassie blue dye for 30 min. The gel was then destained by shaking in water for 2 h with the water being changed every 30 min. The bands were then compared to the weights in the standards lane and the bands for the 33 kDa, 23 kDa, and 18 kDa bands were no longer present in the apo-BBY.

2.8 Conformation of Complete Removal of Manganese via Mn Assay

The following assay was developed by modifying an assay by Semin *[29]*. The assay by Semin was developed by modification of the original assay developed by Serrat *[30]*. This procedure was performed in the dark (or under green light) at 4°C. BBY membrane samples were thawed for 1 hour. Aliquots were taken (35 µg chl of BBY, 5 µg chl of apo-BBY) and suspended in 1 mL buffer A (0.4 M sucrose, 15 mM NaCl, 50 mM MES, pH 6.5) inside of polyethylene microfuge tubes. For the calcium-washed samples, $CaCl_2$ was added to buffer A to a 25 mM

working concentration. The samples were incubated for 2 minutes and then centrifuged at 14 000 Xgs in a bench-top microfuge for 10 minutes. The liquid was then removed from the samples and the pellets were resuspended in 100 µL of 0.6M HCl to extract Mn from the membrane particles. The remainder of this procedure was performed at room temperature under normal lighting. After mixing via Vortex mixer for 1 minute, the samples were diluted to 1 mL and centrifuged in a bench-top microfuge at 14 000 Xgs for 5 minutes to remove the remaining membrane particles. Then the resulting supernatant analyte solution was removed into new microfuge tubes and mixed with 40 µL of 2 M NaOH. The samples were mixed with a vortex mixer for 1 minute and incubated for 15 minutes. The samples were then mixed consecutively with 40 µL of TMB solution (1 mg/mL of 3,3□,5,5□-tetramethylbenzidine in 0.1 M HCl) and 40 µL of 5.3 M phosphoric acid. A blank was prepared by mixing 900 µL of 0.06 M HCl with 40 µL each consecutively of 2 M NaOH, TMB solution and 5.3 M phosphoric acid. The samples were then analyzed at 450 nm using a UV-Vis spectrometer. The assay and instrument were standardized by analyzing standard solutions of $MnCl_2$. The extinction coefficient at 450 nm for Mn determined using the TMB reaction on standard solutions of Mn was 2.4668×10^{-2} $\mu mol^{-1}\cdot cm^{-1}\cdot L$.

3. Results and Discussion

In order to gain a more complete understanding of photoassembly, the temperature dependence of both the intact PSII and OEC-depleted PSII had to be explored. The two processes, oxygen evolution and photoassembly, were found to have a shared maxima of 28 °C. From there, the effect of $K_3[Fe(CN)_6]$ and flash number and flash frequency were explored, and it was found that $K_3[Fe(CN)_6]$ has a detrimental effect at higher temperatures. It was also determined that, under oxidant limiting conditions, photoassembly is acceptor side limited. Some

of the frequency experiments reproduced previous experiments and showed that, under high light conditions, photoassembly is inhibited. Protease activity was also found to be present in the temperature range from 30-35 °C while conducting photoassembly experiments, and was overcome with addition of fresh Calbiochem protease inhibitor cocktail. This protease inhibitor cocktail contained: AEBSF, Hydrochloride, Aprotinin, Bovine Lung, E-64 Protease inhibitor, Leupeptin, Hemisulfate all of which were used to inhibit the Serine, Cysteine, and Trypsin-like proteases.

The results for the standardization of the Mn assay are organized into Table 1. The results for Mn content of BBY and apo-BBY particles are organized into Table 2. The results for the determination of Chl (and PSII) content of BBY and apo-BBY used to calculate Mn per PSII is organized into Table 3.

3.1 Oxygen Evolution

Figure 9 represents the graph that is generated by the oxygraph when recording the oxygen production by the sample. The slope of the increase is determined and then used to calculate the rate of oxygen evolution in O_2 evolution rate (µmol O_2/mg Chl *a*/h).

In order to first determine the optimal conditions for testing oxygen evolution, experiments were conducted to optimize the concentration of ($K_3[Fe(CN)_6]$) (Fig 10.), $K_3[Fe(CN)_6]$ is the primary electron acceptor used to replace the plastoquinones which naturally accept the electrons from PSII. From this, an optimal concentration of 1 mM was determined to be sufficient for the following oxygen evolution experiments; however, for photoassembly, 5 mM was found to be necessary for the optimal photoassembly and the oxygen evolution measurement to follow. As it can be seen in Figure 9, there is no discernible difference between

1 and 5 mM of $K_3[Fe(CN)_6$ for oxygen evolution. In order to carry out any experiments, the most optimal concentration of $K_3[Fe(CN)_6]$ had to be determined and then utilized, so that maximum oxygen evolution could be measured. In addition, the potential for detrimental effects had to be explored. Since there was no benefit to using any concentration higher that 1 mM, initial experiments were conducted using 1 mM $K_3[Fe(CN)_6]$. The 5 mM was consistent with the concentration used by the Dau group, but there have been other groups using 1 mM $K_3[Fe(CN)_6]$ for their electron acceptor *[2]*.

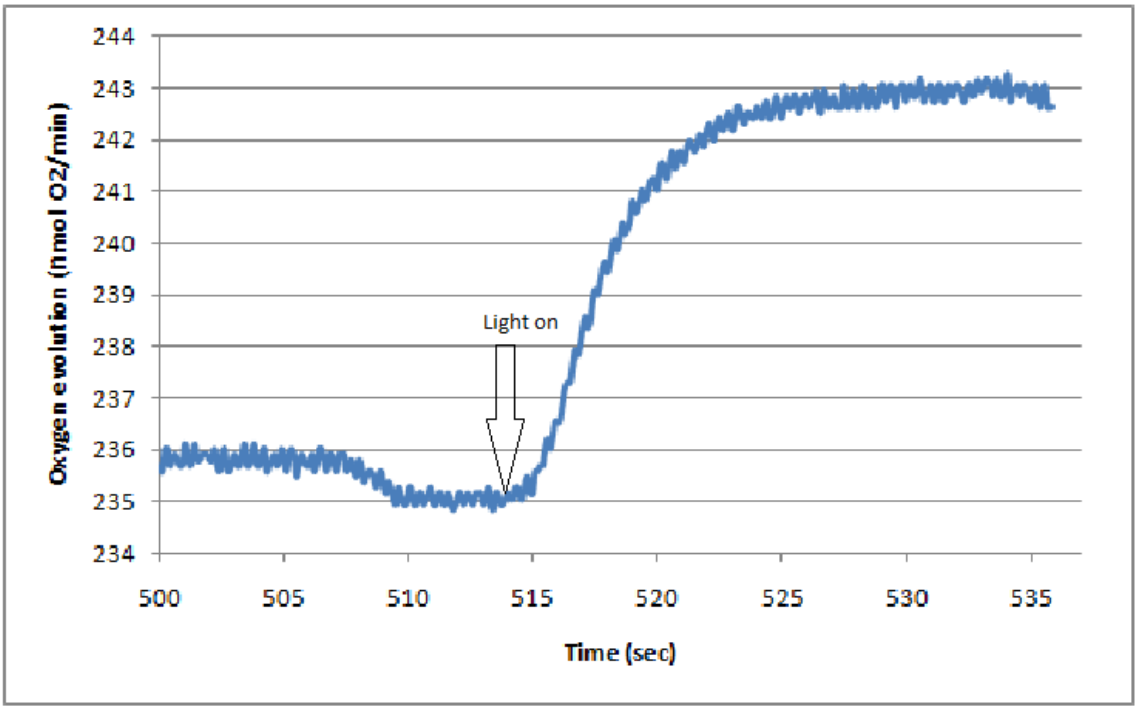

Figure 9. Oxygen evolution graph in nmol of O_2 in seconds for BBYs at a concentration of 5 mM $K_3[Fe(CN)_6]$ and 750 µE of illumination. The initial rate of oxygen evolution was determined by taking the slope of the trace following introduction of the actinic light.

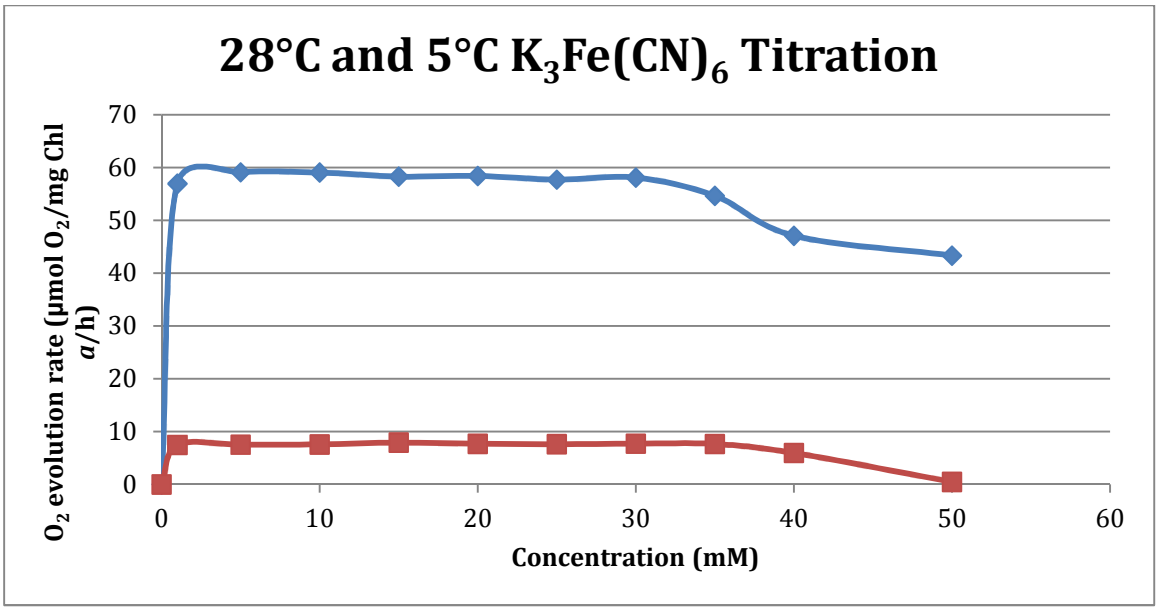

Figure 10. A [$K_3Fe(CN)_6$] titration at the temperature 28 °C (blue diamonds) and at a low temperature 5 °C (red squares). Experiments were conducted using BBYs with a concentration of 12.5 µg/ml [Chl *a*] and an illumination intensity of 750 µE from prep 1 (12/11/11).

Once optimal parameters were established for the $K_3[Fe(CN)_6]$ concentrations, the conditions had to be established using the redox mediator DCBQ (Figure 11.). DCBQ is a redox mediator that is soluble in both the lipid membrane and water, and, because it is a quinone without a tail, it can freely partition into and out of the membrane. It is thusly able to accept electrons from the Q_B site of PSII and then donate the electron to the terminal electron accepter $K_3[Fe(CN)_6]$. An optimal concentration of 150 µM was decided upon for the temperature dependence curve of oxygen evolution from the titration of DCBQ concentration in Figure 11. From the oxygen evolution experiments both in the presence and in the absence of DCBQ (Figure 12.), a conserved temperature maximum of 28 °C was observed, with the DCBQ increasing the rate of oxygen evolution 6 fold. The increase in the rate of oxygen evolution in the presence of DCBQ is due to the fact that DCBQ is a quinone and acts as a redox mediator that

can partition into the membrane and accept electrons and then pass them onto $K_3[Fe(CN)_6]$ with a high efficiency. This increase, when compared to the normalized rate of oxygen evolution of BBYs without DCBQ, a change in the temperature profile for the temperature dependence of PSII was observed. The change in the temperature profile is due to the effect that DCBQ has on the efficiency of electron transfer. Because DCBQ is more easily able to accept and transport electrons to the $K_3[Fe(CN)_6]$ at the lower temperatures, it flattens and broadens out the temperature curve. The change in profile is due to the DCBQ's ability to overcome some of the efficiency loss at the lower temperatures. The observed maximum was consistent with the literature values reported in Schiller and Dau *[2]*. The use of 28 °C was only mentioned by the Dau group and a varying range of temperatures have been used for oxygen evolution measurements. This work is the most comprehensive temperature dependence study that has been conducted on the PSII protein complex.

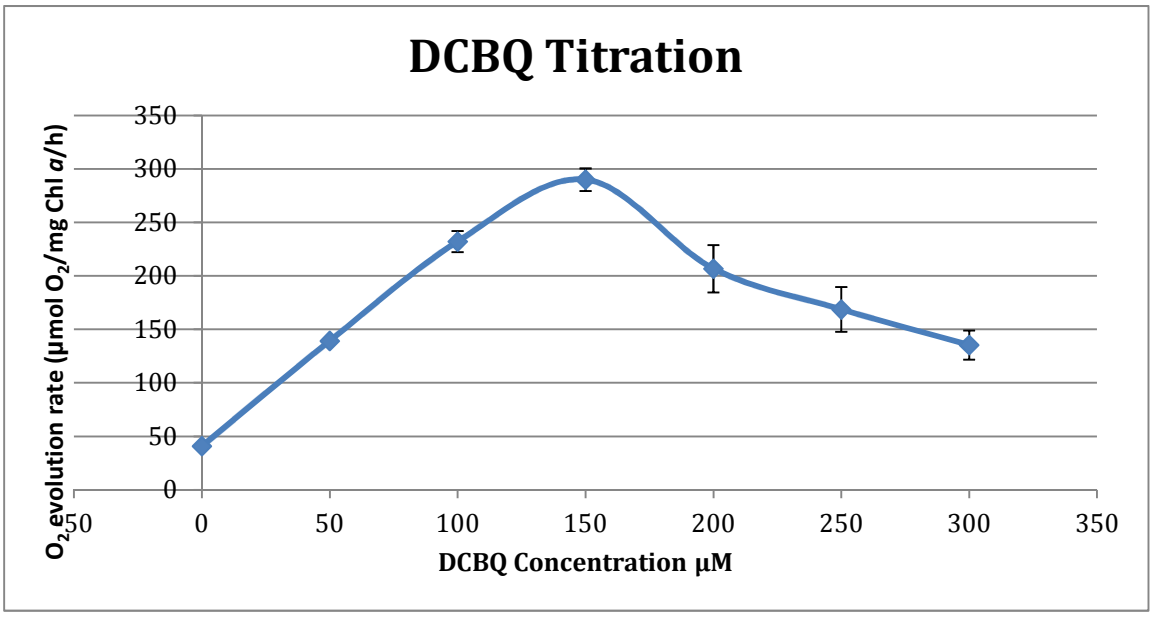

Figure 11. A DCBQ titration at the temperature 28 °C (blue diamonds) Experiments were conducted using BBYs with a concentration of 12.5 µg/ml [Chl *a*] and an illumination intensity of 750 µE from prep 1 (12/11/11).

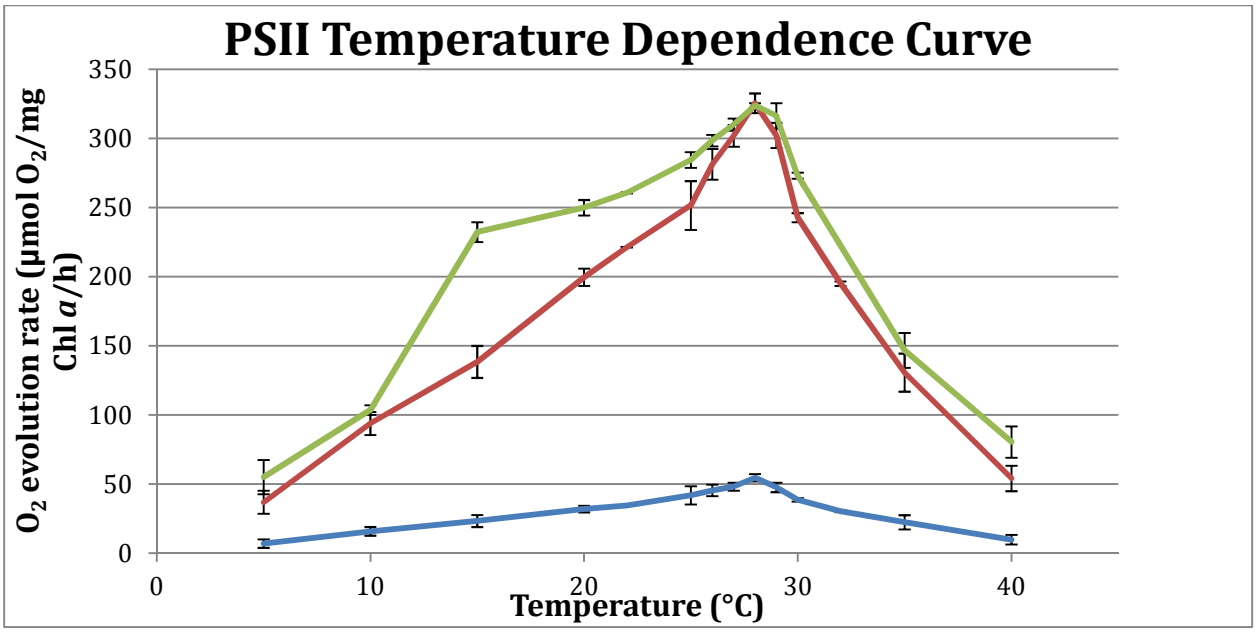

Figure 12. Temperature dependence curve of BBY particles in the presence (green line) and absence (blue line) of DCBQ and with the rates of oxygen evolution normalized (red line). All experiments were conducted using BBYs with a concentration of 12.5 µg/ml [Chl *a*] and an illumination intensity of 750 µE from prep 1 (12/11/11). All points have an n of 3 except for 28 °C which has an n of 5.

3.2 Photoassembly

Once the temperature maximum for oxygen evolution had been established, we looked at the temperature dependence of the photoassembly process. Apo-BBYs were made via the procedure described in methods and were then photoassembled using the procedure described in methods, photoassembly was done at the temperature range of 5–40 °C, Figures 13 and 14, with all oxygen measurements being taken at 28 °C. A temperature maximum of 28 °C was observed for photoassembly as well as oxygen evolution. The same temperature profile for both processes was observed, meaning that the processes are dependent upon the same limiting factor. From Figure 13 and Figure 14 the shared maximum of oxygen evolution of PSII and that of photoassembly can clearly be seen, which indicated that both oxygen evolution and

photoassembly are at their most efficient at 28 °C. This temperature curve is also clear evidence that, whereas most experiments in other labs are conducted at 25 °C, much better signals could be obtained if the experiments would be conducted at 28 °C.

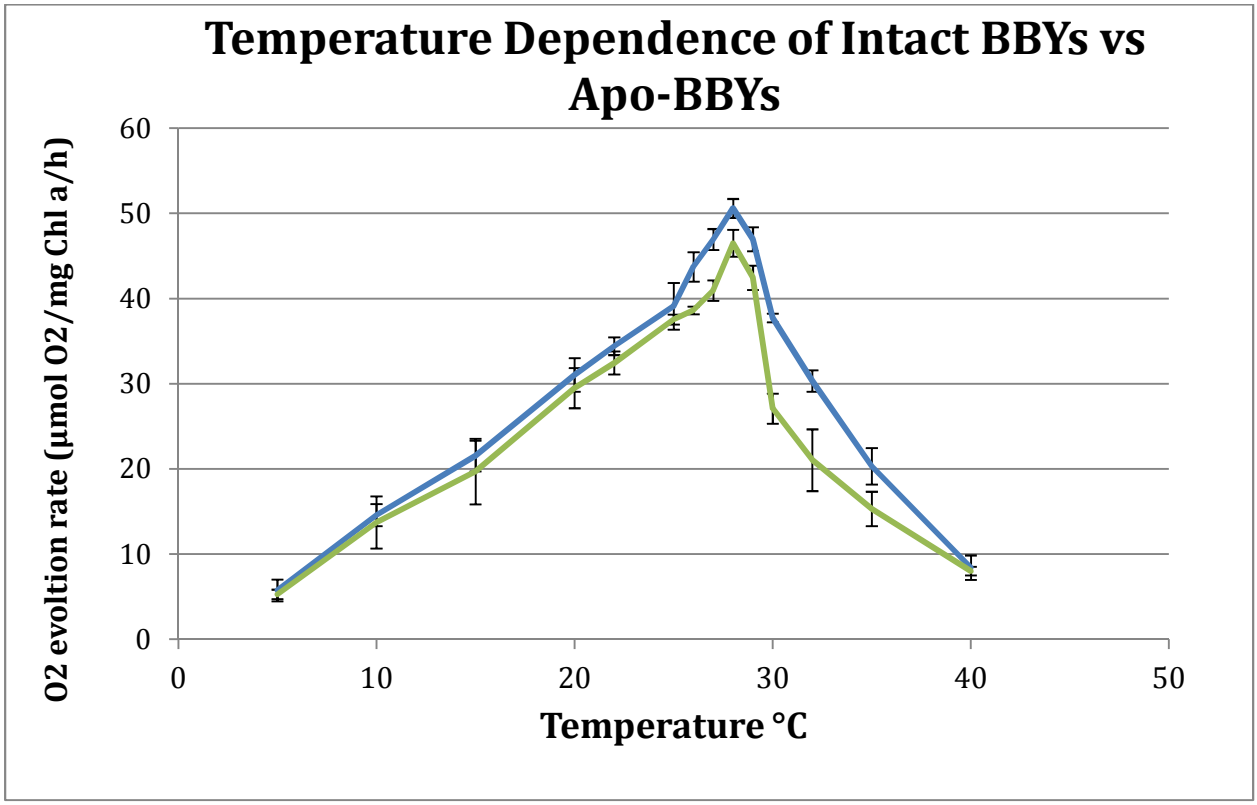

Figure 13. A comparison of the temperature dependence titration for OEC depleted (apo-BBYs) (green line) and intact BBY particles (blue line). Apo-BBYs were made using a pH 9.5 CHES buffer and reassembly of the cluster was done using 200 µl $CaCl_2$ (stock 10 mM), 100 µL of $K_3[Fe(CN)_6]$ (stock 50 mM), 50 µL of $MnCl_2$ (stock 2 mM), 50 µL of sodium bicarbonate (stock 20 mM), 5 µL of apo-BBY (stock 2.5 mg/mL), and 595 µL of K3, with a final volume of 1 mL. Actinic pulsed light at a rate of 100 per min for 10 min experiments were conducted using BBYs at a concentration of 12.5 µg/ml [Chl *a*] and an illumination intensity of 750 µE from prep 1 (12/11/11). All points have an n value of 3 except for 28 °C which has an n value of 5 and in the absence of protease inhibitor cocktail.

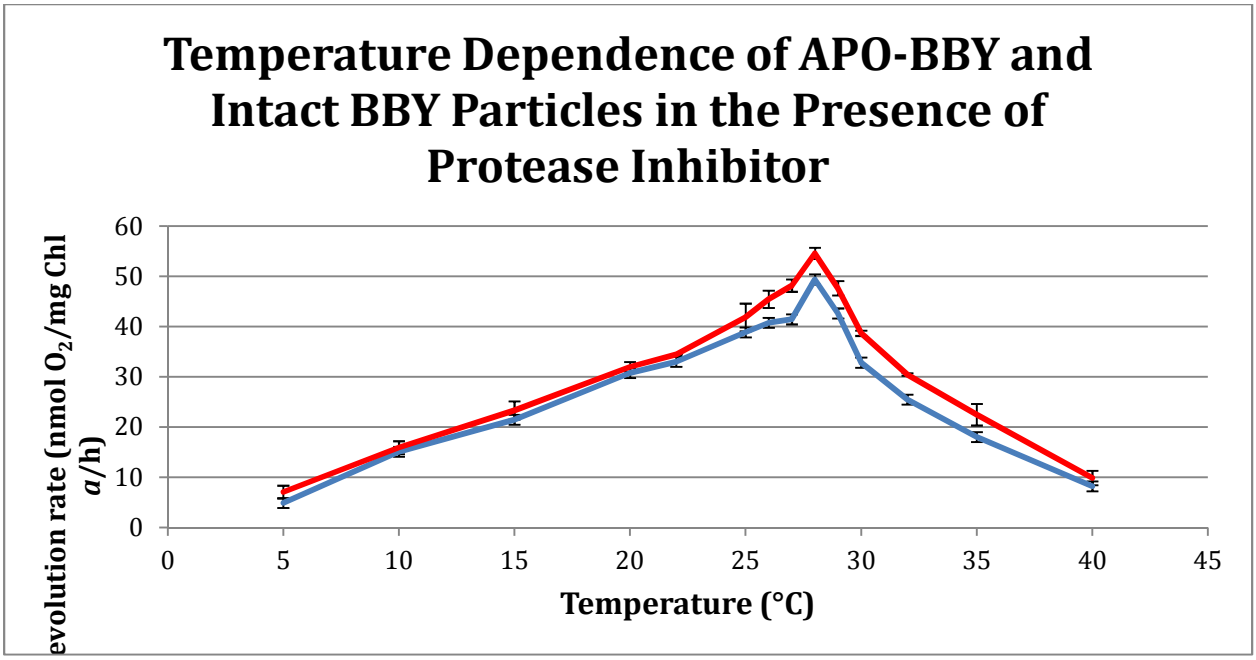

Figure 14. A comparison of the temperature dependence titration for OEC depleted (apo-BBYs) (green line) and intact BBY particles (blue line). Apo-BBYs were made using a pH 9.5 CHES buffer and reassembly of the cluster was done using 200 µl $CaCl_2$ (stock 10 mM), 100 µL of $K_3[Fe(CN)_6]$ (stock 50 mM), 50 µL of $MnCl_2$ (stock 2 mM), 50 µL of sodium bicarbonate (stock 20 mM), 5 µL of apo-BBY (stock 2.5 mg/mL), and 595 µL of K3, with a final volume of 1 mL. Actinic pulsed light at a rate of 100 per min for 10 min experiments were conducted using BBYs at a concentration of 12.5 µg/ml [Chl *a*] and an illumination intensity of 750 µE from prep 1 (12/11/11). All points have an n value of 3 except for 28 °C which has an n value of 5 and in the presence of protease inhibitor cocktail.

Decreased recovery of oxygen evolution between the temperatures of 30-35 °C was observed in Figures 13 and 15. The loss of activity in this temperature range was theorized to be due to protease activity, a protease inhibitor cocktail was added to the mixture and the experiments were repeated. This degradation was prevented by the addition of protease inhibitor cocktail (Fig. 14 and 15), and in the presence of the protease inhibitor cocktail allowed over 90% recovery of oxygen evolution rates at all temperatures measured. This result was the first reported evidence of the temperature dependence of the protease activity. Degradation experiments were also conducted to see what the effects of time and temperature were on the

intact BBYs. From Figure 17 it can be seen that at 28 °C there is 4.5% loss in activity in the proteins if they are left exposed to this temperature for only 5 minutes and increases to 14.7% if exposed for 20 minutes. This however goes from 4.5% to 15.1% and from 14.7% to 49.3% loss in activity when the temperature is raised to 35 °C. This degradation is due to the protease degrading the PSII protein complex during the incubation. Thus, the time treated could greatly affect the amount of activity that would be recoverable, and that all possible steps to limit the time of treatment would need to be taken. This degradation was most likely due to the native chloroplastic proteases, FtsH and Deg, that are present in the thylakoid membrane surrounding PSII. The Deg proteases main function is to mediate the repair of PSII in intact chloroplasts. FtsH is responsible for cleaving the carboxy terminus of the D1 and activating the subunit after it is formed. Deg is responsible for degrading the D1 subunit when it has been damaged during photoinhibition *[31]*.

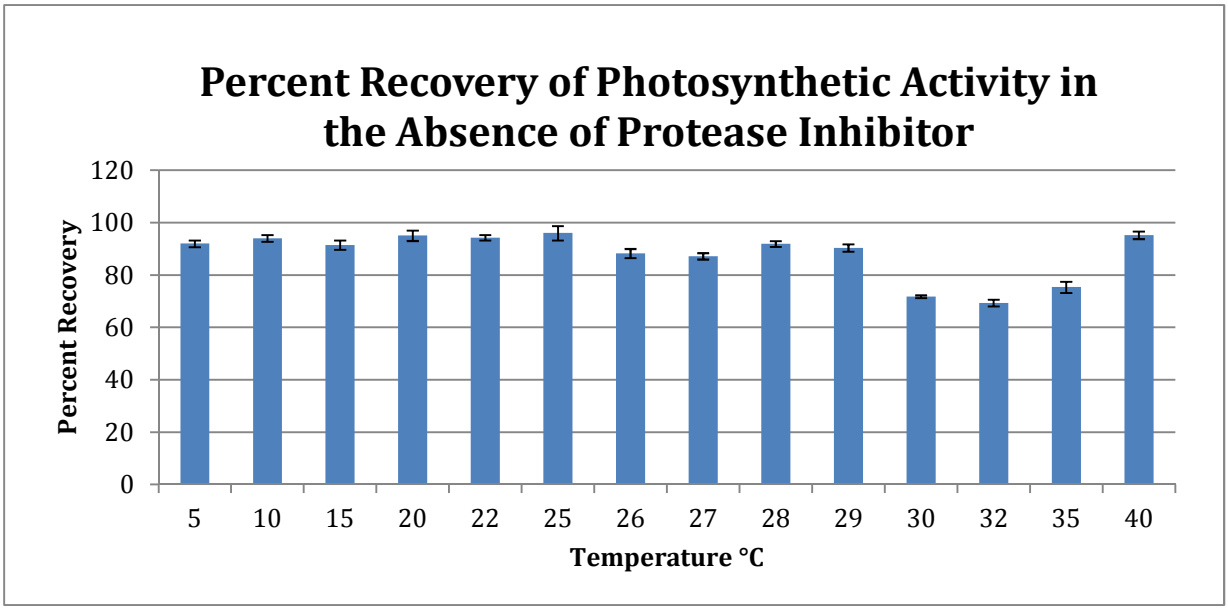

Figure 15. Percent Recovery of oxygen evolution rates for the apo-BBY particles. Experiments were conducted using BBYs with a concentration of 2.5 mg/mL [Chl *a*] (stock) and a working concentration of 5 µg/ml using prep 1 (12/11/11). Photoassembly was conducted as described in Figure 13. All points have an n value of 3 except for 28 °C which has an n value of 5

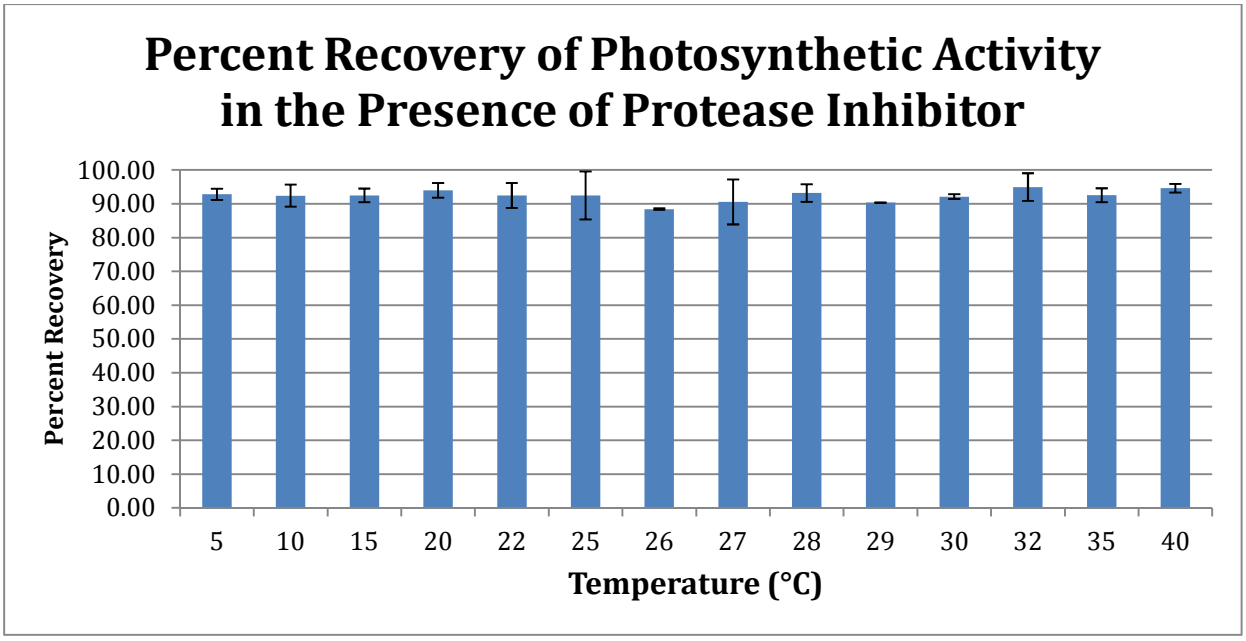

Figure 16. Percent recovery of oxygen evolution rates for the apo-BBY particles when treated with protease inhibitor cocktail. Experiments were conducted using BBYs with a concentration of 12.5 µg/ml [Chl *a*] and an illumination intensity of 750 µE using prep 1 (12/11/11). Photoassembly was conducted as described in Figure 13. All points have an n of 3 except for 28 °C which has an n value of 5.

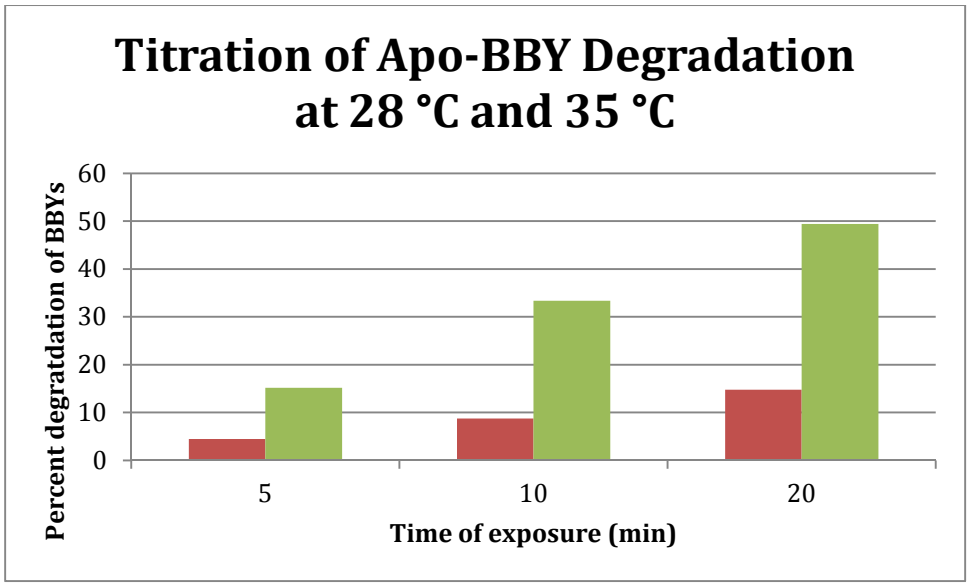

Figure 17. Degradation experiments in which apo-BBYs were incubated that 28 °C (red bar) and then at 35 °C for the specified times with measurements of oxygen evolution.

Photoassembly experiments were conducted with the addition of DCBQ; however, this was found to reduce the manganese oxidation state in the OEC by donating the electrons back to the cluster instead of to the $K_3[Fe(CN)_6]$ and would not allow for photoassembly to take place when the extrinsic proteins were removed. Controls were performed to ensure that the $K_3[Fe(CN)_6]$ was not having a negative effect on the photoassembly or oxygen evolution (Figure 18). It was during this time that the following question arose: could the photoassembly process be using up most of the 1 mM $K_3[Fe(CN)_6]$ during the pulsed light treatment leaving the sample with a lower than ideal oxidant concentration. To test the effect of $K_3[Fe(CN)_6]$, a series of controls were done using not only different flash frequencies and flash numbers but also different concentrations of $K_3[Fe(CN)_6]$ to determine the effects that it would have on photoassembly.

The first control was to investigate whether increasing the number of flashes would have any effect on the amount of OEC clusters that reassembled (Figure 19). The decrease in activity as one moves away from the temperature maximum is due to the change in charge separation of the OEC at different temperatures. It has been observed that as the temperature is decreased, the ability of $P680^+$ to transfer electrons was reduced and causing a decrease in the OEC's ability to function *[32]*. From there, a series of flash controls was performed to ascertain that all conditions had been optimized to produce the highest rates of oxygen evolution and to ensure that $K_3[Fe(CN)_6]$ was not interfering under any of the testing conditions. In experiments conducted at the temperature maximum, 28 °C (Figure 20), $K_3[Fe(CN)_6]$ was found to have no detrimental effect at any of the tested concentrations or over the span of 2000 flashes at a rate of 100 per minute. This was in line with previous experiments on intact PSII which indicated that at 28 °C, the oxygen evolution rates would not be increased by the addition of more $K_3[Fe(CN)_6]$. At 5 °C (Figure 21) oxygen evolution was found to be at the highest rates if 5 mM $K_3[Fe(CN)_6]$ was

administered with at least 1000 flashes. There were detrimental side effects to having higher concentrations. However, at 40 °C (Figure 22), $K_3[Fe(CN)_6]$ was found to be detrimental if the photoassembly mixture was exposed for longer than 1000 flashes at 5 mM $K_3[Fe(CN)_6]$. $K_3[Fe(CN)_6]$ was detrimental to PSII if administered at 10 mM for any amount of flashes. Figures 21 and 22 show the first experimental data showing that with the addition of excess $K_3[Fe(CN)_6]$, the inherent inefficiencies of photoassembly could be overcome and the maximum oxygen evolution rate could be maintained throughout the entire temperature curve.

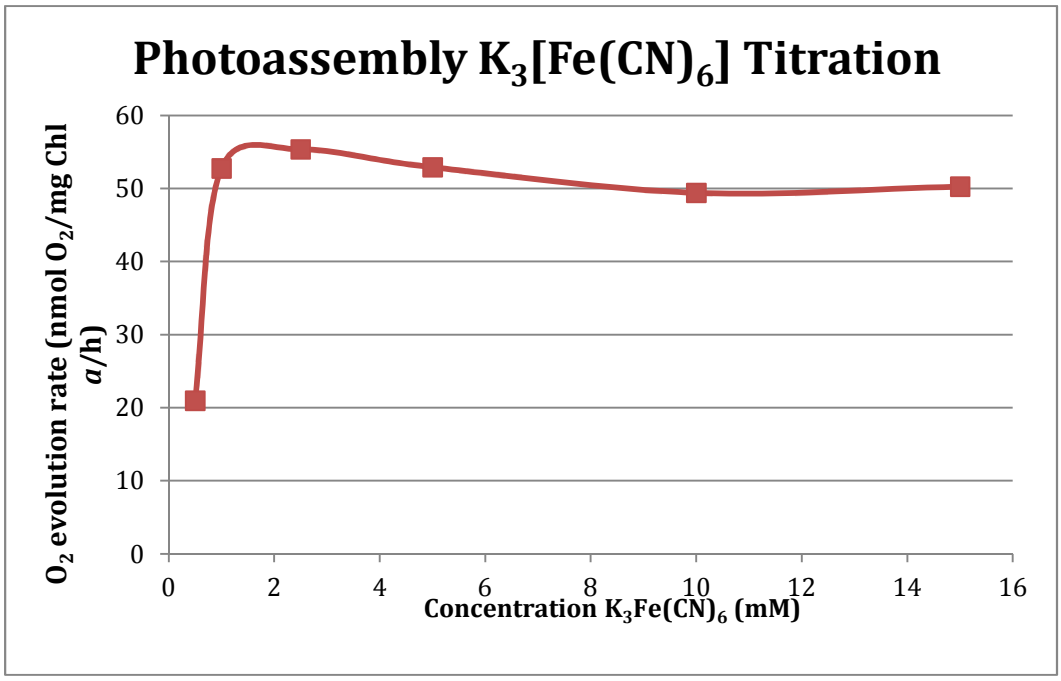

Figure 18. A $[K_3Fe(CN)_6]$ titration at the temperature maxima of 28°C. Experiments were conducted using BBYs with a concentration of 12.5 µg/ml [Chl *a*] and an illumination intensity of 750 µE using prep 1 (12/11/11). Photoassembly was conducted as described in Figure 13 and in the presence of protease inhibitor cocktail.

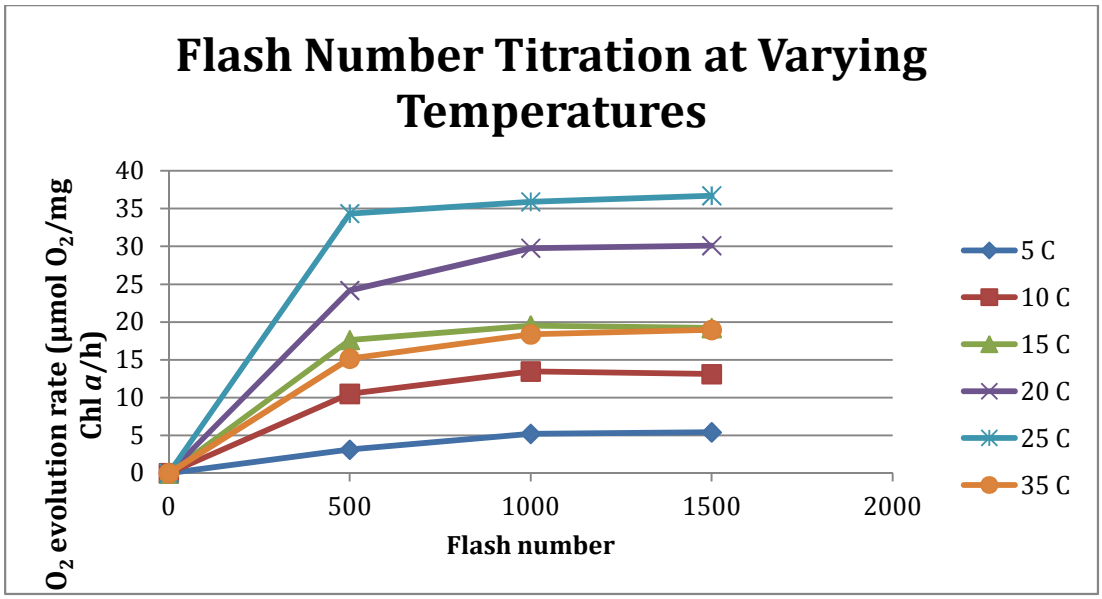

Figure 19. A flash titration of the photoassembly of apo-BBYs oxygen evolution rates with 1 mM $K_3[Fe(CN)_6]$ using photoassembly procedures described in Fig. 13. The titration was performed at 5 °C (blue diamond), 10 °C (red square), 15 °C (green triangle), 20 °C (purple X), 25 °C (blue *), and 35 °C (orange circle). Experiments were conducted using apo-BBYs with a concentration of 12.5 µg/ml [Chl *a*] and an illumination intensity of 750 µE using prep 2 (5/14/12) in the presence of protease inhibitor cocktail.

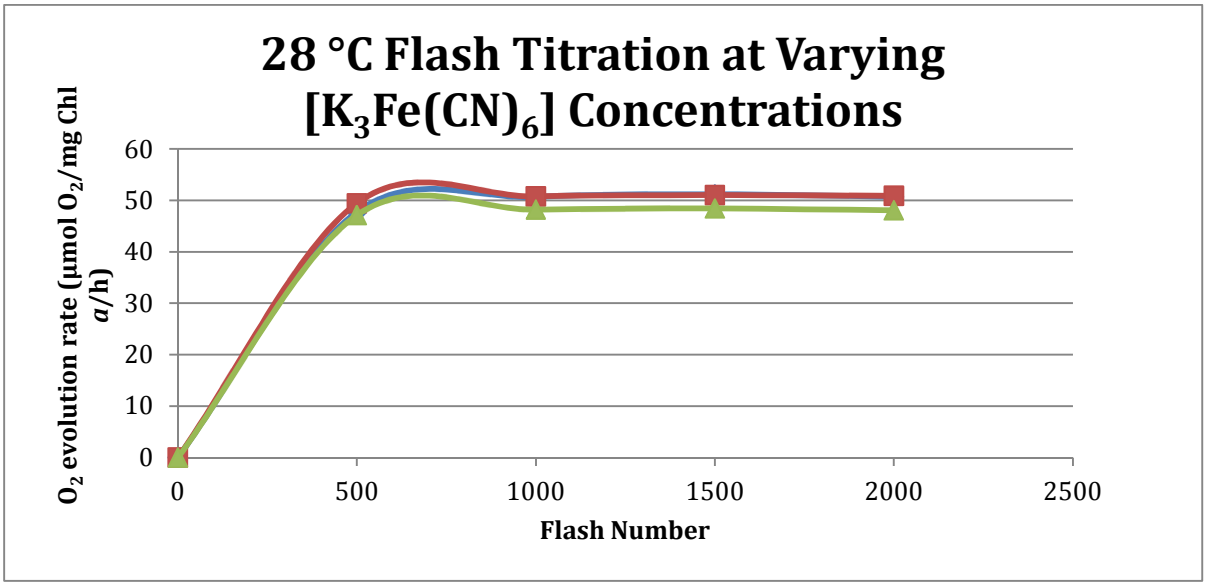

Figure 20. Flash titration of oxygen evolution rates at 1 mM (blue diamonds), 5 mM (red squares), and 10 mM (green triangles) $[K_3Fe(CN)_6]$. Experiments were conducted using apo-BBYs with a concentration of 12.5 µg/ml [Chl *a*] and an illumination intensity of 750 µE using prep 2 (5/14/12). Photoassembly was conducted as described in Figure 13 and in the presence of protease inhibitor cocktail.

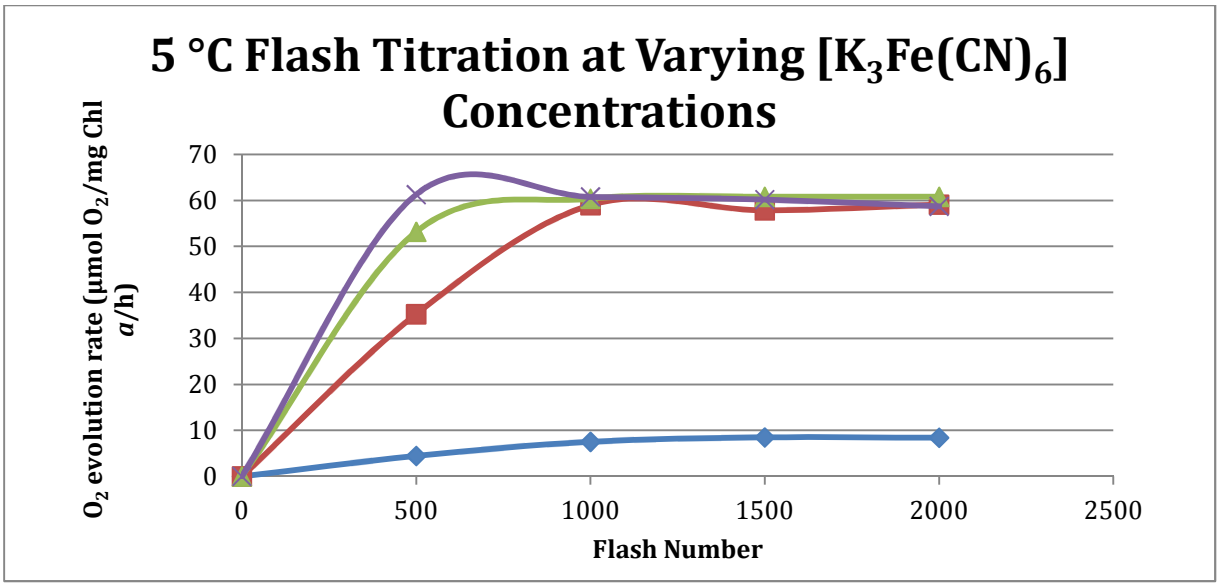

Figure 21. A 5 °C flash titration of oxygen evolution rates at 1 mM (blue diamonds), 5 mM (red squares), 10 mM (green triangles), and 15 mM (purple plus signs) [$K_3Fe(CN)_6$]. Experiments were conducted using apo-BBYs with a concentration of 12.5 µg/ml [Chl *a*] and an illumination intensity of 750 µE using prep 3 (10/13/12). Photoassembly was conducted as described in Figure 13 and in the presence of protease inhibitor cocktail.

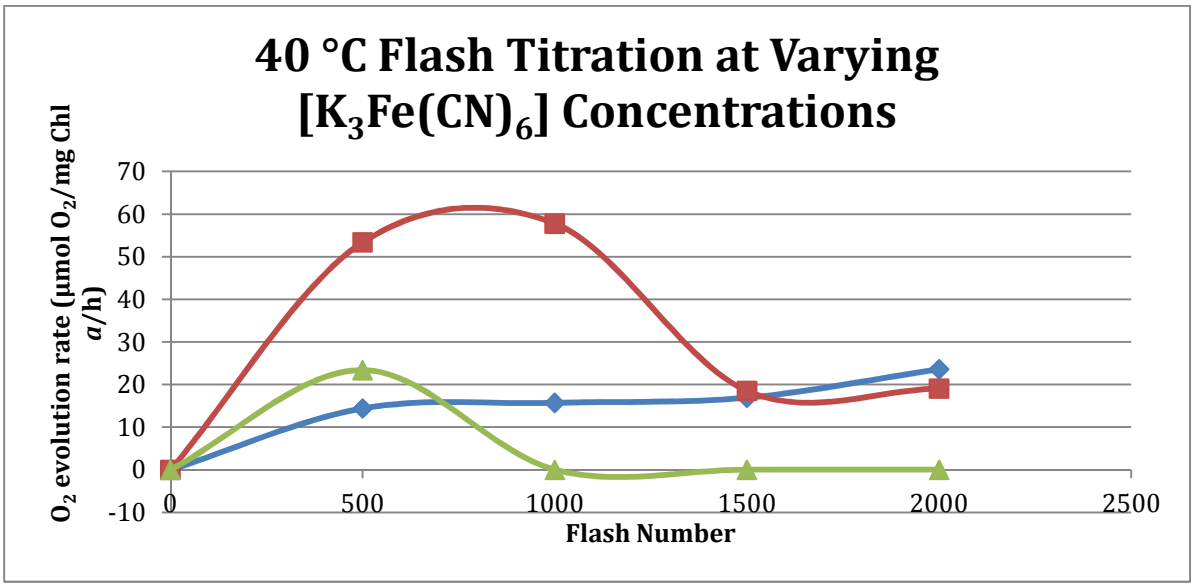

Figure 22. 40 °C flash titration of oxygen evolution rates at 1 mM (blue diamond), 5 mM (red square), and 10 mM (green triangle) [$K_3Fe(CN)_6$]. Experiments were conducted using apo-BBYs with a concentration of 12.5 µg/ml [Chl *a*] and an illumination intensity of 750 µE using prep 3 (10/13/12). Photoassembly was conducted as described in Figure 13 and in the presence of protease inhibitor cocktail.

It was also necessary to test the effect of the frequency at which the flashes were being delivered as well and to see if the concentration of $K_3[Fe(CN)_6]$ was having any effect (Figure 23). The results from Figure 23 confirm observations in the literature stating that under high continuous light, photoassembly is not able to take place. The cluster is not able to form the first intermediate under these conditions, meaning that at least some dark step is required in order to assemble the OEC. As the experiments were conducted, it became clear that 100 flashes per minute was the best for the strobe system that was used and for any concentration of $K_3[Fe(CN)_6]$ at 28 °C. Because it was becoming clear that 5mM would provide better oxygen evolution rates for the photoassembled BBYs, a frequency titration was performed at 5, 28, and 40 °C (Fig 24) to explore the potential that the $K_3[Fe(CN)_6]$ would behave less efficiently at the extreme ends of the temperature curve. 5 mM $K_3[Fe(CN)_6]$ was found to be beneficial at the far ends of the temperature curve when the apo-BBYs were exposed to higher frequency flashes, but even with the effect, it was still found that 100 flashes per minute would be adequate when using 5 mM $K_3[Fe(CN)_6]$ at any temperature along the curve.

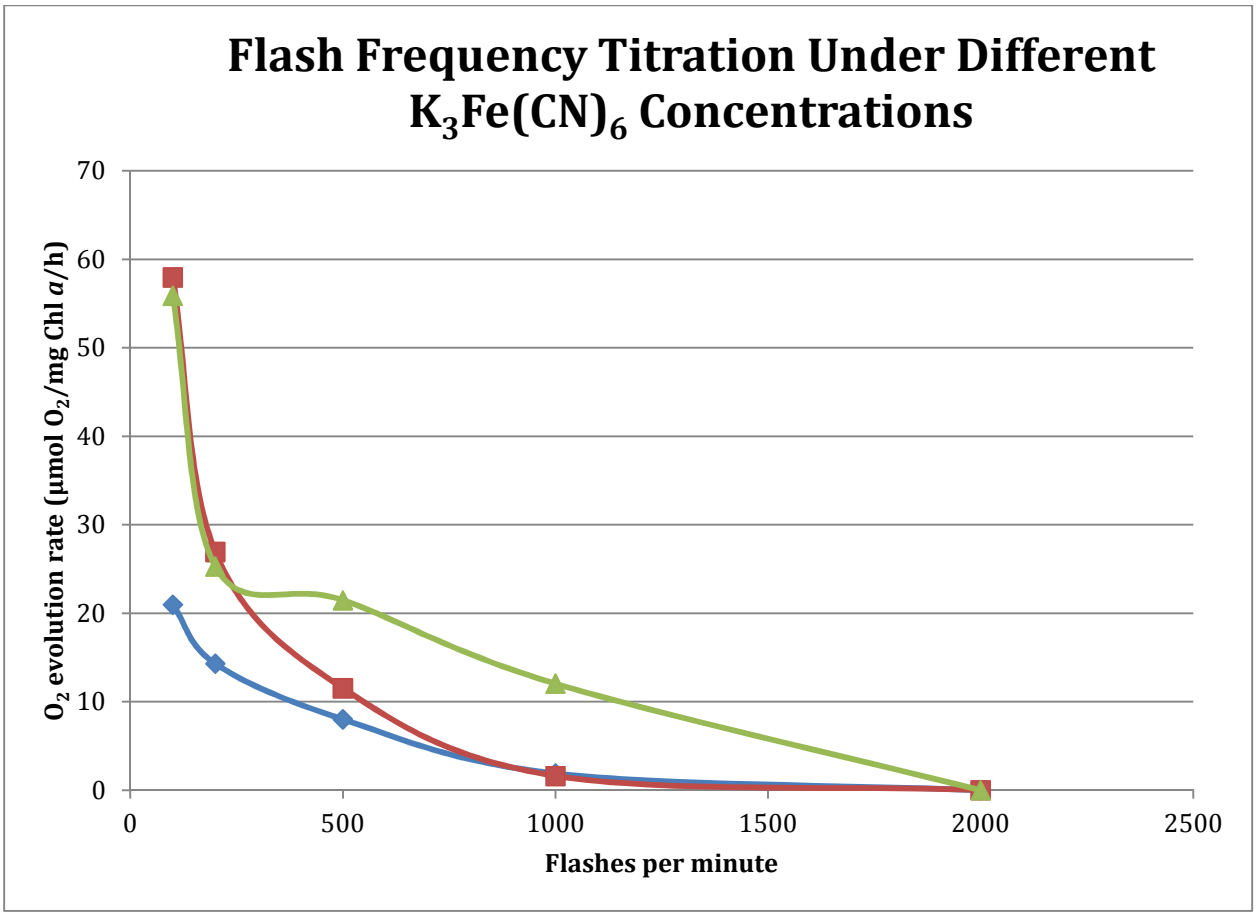

Figure 23. A flash frequency titration of oxygen evolution rates under different $K_3Fe(CN)_6$ concentrations. [$K_3Fe(CN)_6$] at 0.5 mM (blue diamond), 1 mM (red square), and 5 mM (green triangle). Experiments were conducted using BBYs with a concentration of 12.5 µg/ml [Chl *a*] and an illumination intensity of 750 µE using prep 2 (5/14/12). Photoassembly was conducted as described in Figure 13 and in the presence of protease inhibitor cocktail.

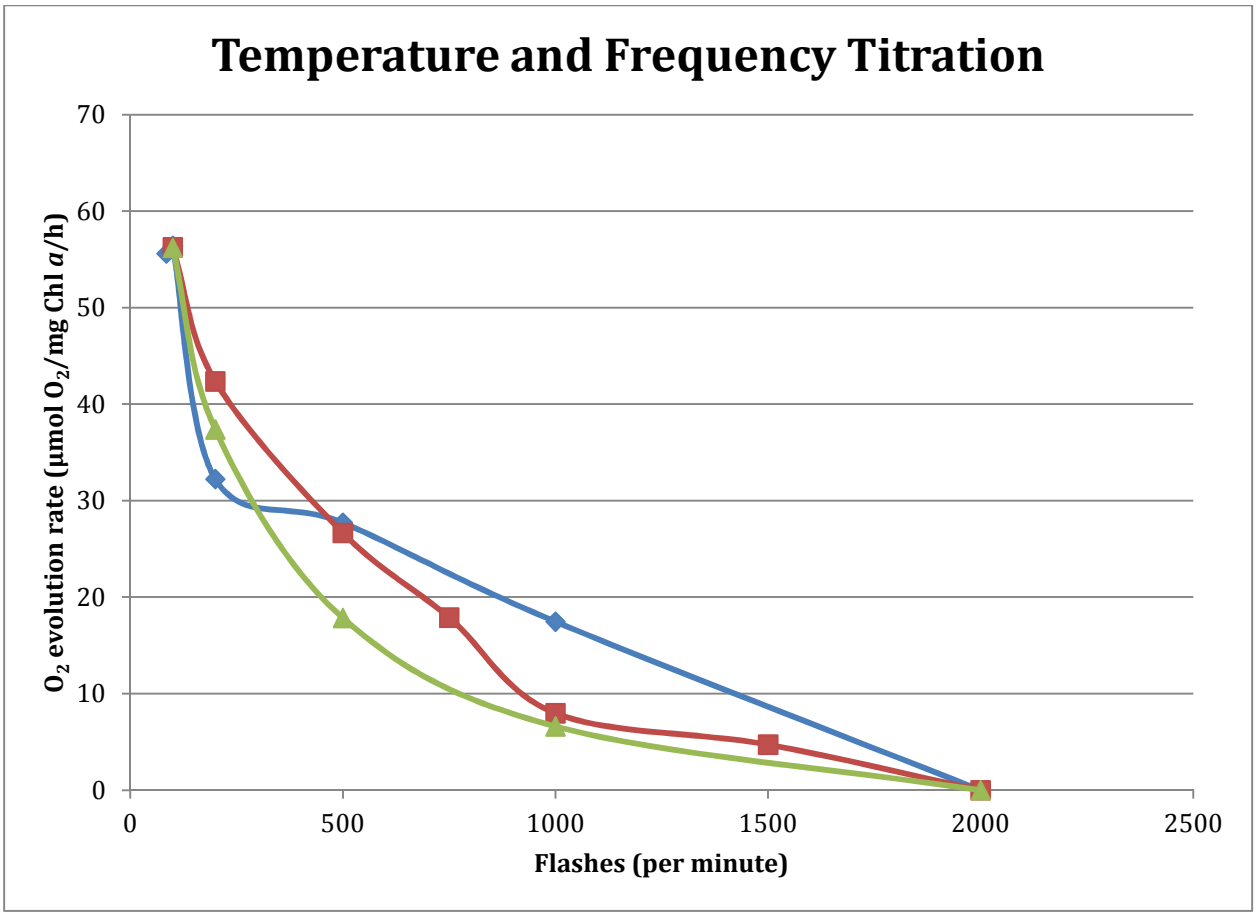

Figure 24. A flash frequency titration of photoassembly oxygen evolution rates using $K_3Fe(CN)_6$ 5 mM at 28 °C(blue diamond), 5 °C (red square), and 40 °C (green triangle). Experiments were conducted using BBYs with a concentration of 12.5 µg/ml [Chl *a*] and an illumination intensity of 750 µE using prep 2 (5/14/12). Photoassembly was conducted as described in Figure 13 and in the presence of protease inhibitor cocktail.

With the new information that 5 mM $K_3[Fe(CN)_6]$ would be able to overcome the inefficiency of photoassembly, new temperature dependence curves were generated using 0.5 mM, 1 mM, 2.5 mM, and 5 mM $K_3[Fe(CN)_6]$ (Fig 25), when using 5 mM $K_3[Fe(CN)_6]$ oxygen evolution rates were found to be maintained at peak amounts throughout the entire curve. It can be concluded by comparing the different concentration curves and the curve of intact BBYs, under oxidant limiting conditions, the temperature profile is the same for intact and photoassembled apo-BBYs. The first piece of information that can be concluded about this

phenomenon is that the photoassembly is an acceptor side limited reaction under oxidant limiting conditions. These are some the most recent experiments exploring the acceptor side of PSII and the potential for the rate limiting step to be in this half of the electron transport pathway.

In an attempt to look at single turnover of the OEC, a series of oxygen evolution experiments were conducted to see if oxygen could be evolved using actinic pulsed light (Fig 26). However, the frequency of the pulses required to generate a measurable amount of oxygen using the Clark type electrode made further experiments in this area impractical.

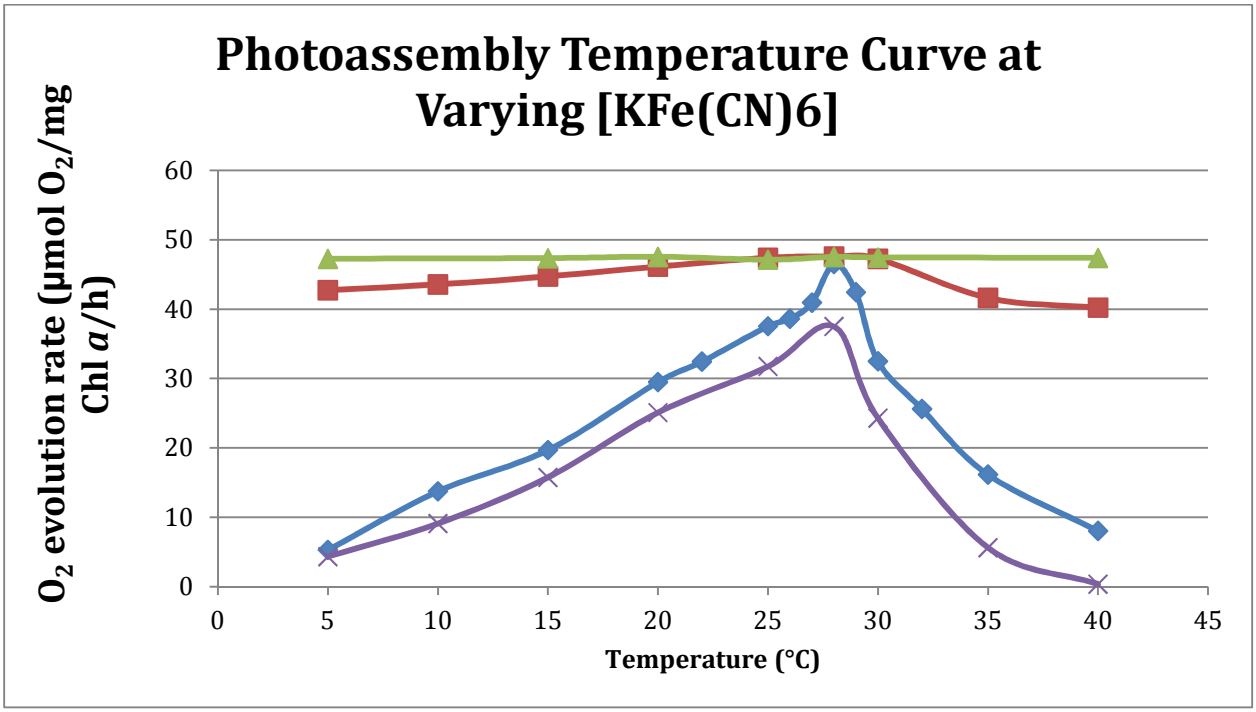

Figure 25. Effect of $[K_3Fe(CN)_6]$ on rates of apo-BBY oxygen evolution. The concentrations tested were 0.5 mM (purple dashes), 1 mM (blue diamonds), 2.5 mM (red squares), and 5 mM (green triangles). Experiments were conducted using BBYs with a concentration of 12.5 µg/ml [Chl *a*] and an illumination intensity of 750 µE using prep 2 (5/14/12). Photoassembly was conducted as described in Figure 7 and in the presence of protease inhibitor cocktail.

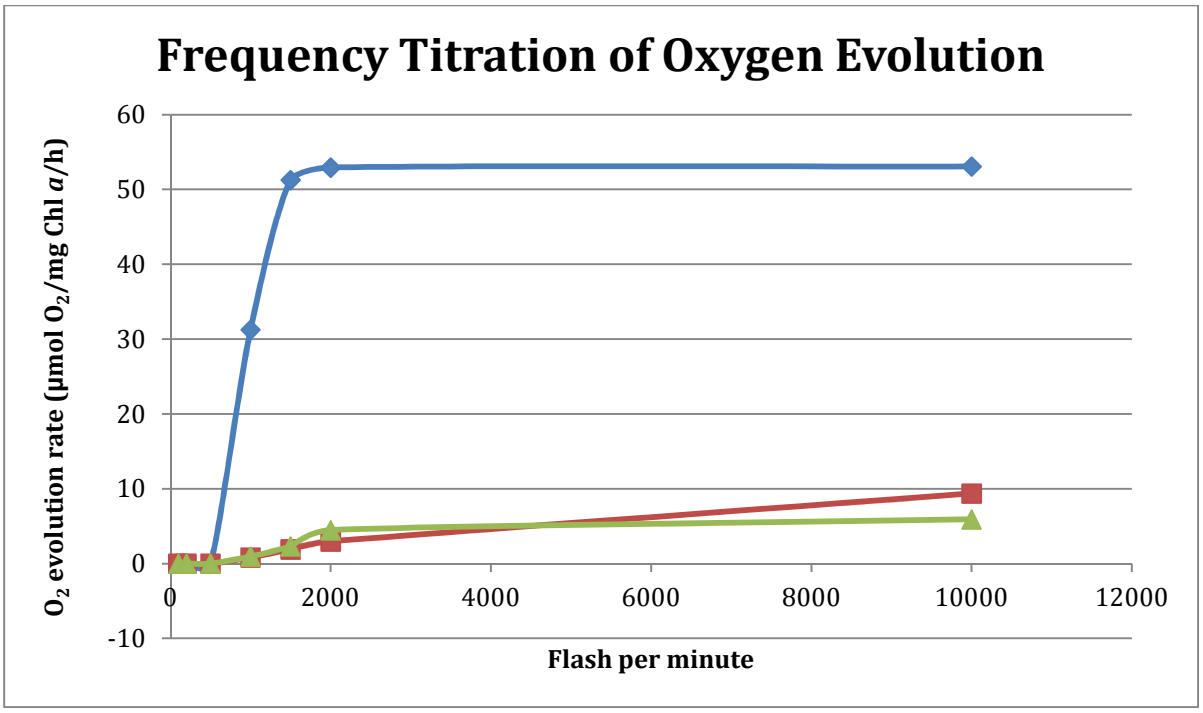

Figure 26. Flash titration at 5 mM [$K_3Fe(CN)_6$] for oxygen evolution of intact BBY particles 28°C (blue diamonds), 5°C (red square), and 40°C (green triangle). Experiments were conducted using BBYs with a concentration of 12.5 µg/ml [Chl *a*] and an illumination intensity of 750 µE from prep 2 (5/14/12) and in the presence of protease inhibitor cocktail.

In order to probe the model for photoassembly proposed first by Cheniae and then by Zaltsman (Fig 27) the dark rearrangement step had to be explored. Experiments were performed in which a 1 s preflash was delivered to a prepared sample of apo-BBYs. Then the sample was allowed to dark adapt and then oxygen evolution was measured (Figure 27). The mechanisms reported by Cheniae stated that only approximately 2 s was needed between flashes to generate the maximum amount of assembled OEC centers. These results lent credence to there being a long dark step and that only 1 second of pre illumination was required to get to an intermediate stage in photoassembly *[33]*. Initial experiments conducted with the 1 s pre-flash indicated that there was at least 1, possibly 2, or more steps between IM_1 and IM^*_1 which are both light sensitive intermediates that have yet to be identified. The older models do not account for the

possibility of light being able to inactivate the formation of the OEC, our high light experiments show that this occurs and so there must be a light sensitive intermediate that has not been accounted for it the old models. Figure 27 is our proposed model for photoassembly; this new model would reconcile that data shown by Cheniae and Zaltsman as well as include the new results we obtained from the 1 s pre-flash experiments. From Figures 23 and 24 it can be seen that high continuous light causes the inactivation of the OEC, which supports the idea of a light dependent intermediate that is not presented in Figure 7. Under pulsed light or 1 s pre-flash, we were able to populate IM_1 which then underwent a slow dark rearrangement which we were able titrate. This rate constant would have been k_2 which as defined, is a macro rate constant. Figure 28 showed an essential dark step that if exposed to light caused the intermediate to go to a nonfunctional state. This state was then able to reset back to IM_0, allowing it to try to assemble correctly. The 1 s pre-flash was a repeat of work done by Kolling *[27]*, and was significant because it was a 1 s photon pulse as opposed to the train of pulses that was normally used to perform photoassembly. Because this illumination period was just 1 exposure to light followed by the dark adaptation step, the dark rearrangement kinetics can truly be probed whereas the pulse train does not allow for this. This new model brings together the work done by Cheniae on the rate constant k_D and shows a more viable way for the cluster to reset and try to reassemble. Zaltsman's work on k_2 and our work on exploring k_2 are in agreement, and this new model unifies all of the previous work and presents a much more accurate model for what is occurring in photoassembly *[4,34,35]*.

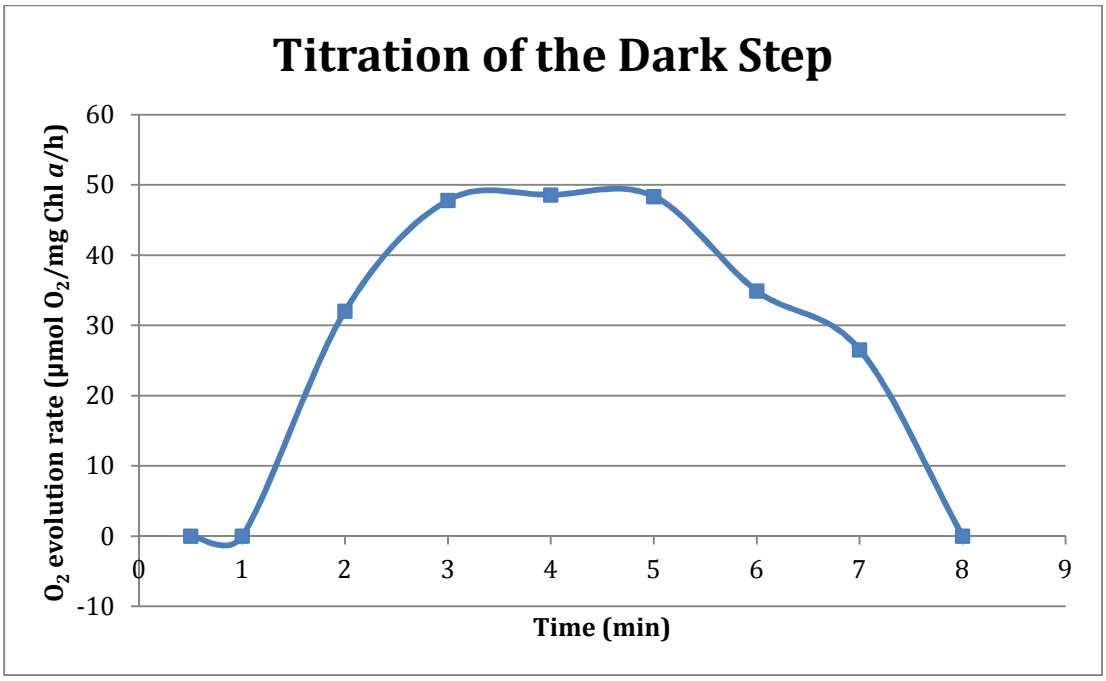

Figure 27. A titration of the dark step of photoassembly using a 1 second pre flash. Experiments were conducted using BBYs with a concentration of 12.5 µg/ml [Chl *a*] and an illumination intensity of 750 µE using prep 3 (10/13/12) and in the presence of protease inhibitor cocktail.

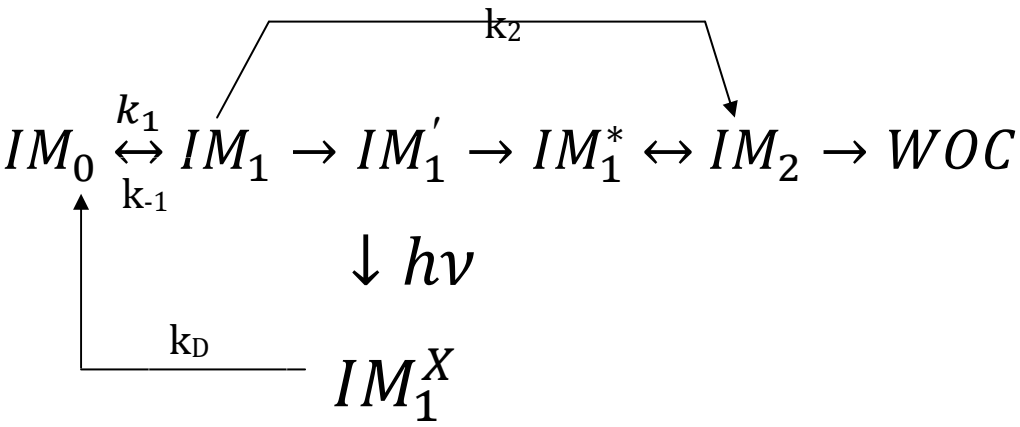

Figure 28. Newly proposed model for photoassembly that incorporates both traditional models as well and the data relating to the inactivation under highlight conditions.

Summary

This study has described the first detailed mapping of the temperature dependence of both oxygen evolution and photoassembly. It was shown that through the addition of the redox mediator DCBQ, a 6 fold increase was observed as well as a broadening of the temperature curve at lower temperatures due to the DCBQ's ability to overcome inefficiencies in the electron transport pathway of PSII. DCBQ was found to inhibit photoassembly owing to its ability to transfer electrons back to the exposed OEC and re-reducing the cluster so that it was unable to form*[35]*. OEC depleted apo-BBYs were formed using a CHES pH 9.5 treatment to remove the extrinsic proteins and the OEC. This was confirmed by SDS-PAGE gel and Mn assay. The temperature maximum for both oxygen evolution and photoassembly was found to be 28 °C and they shared the same temperature profile when protease inhibitor cocktail was present. Through the series of experiments investigating the effect of $K_3Fe(CN)_6$ and frequency all aspects of the photoassembly were optimized to provide the best rates possible for kinetic studies. It was found that 5 mM $K_3Fe(CN)_6$ with actinic flashes administered at a rate of 100 per min with a total of 1000 flashes provided more than adequate rates. Through the experiments conducted using varying concentrations of $K_3Fe(CN)_6$ it was concluded that the earlier temperature profile was under oxidant limiting conditions and could be overcome with the addition of sufficient $K_3Fe(CN)_6$ and at 5 mM the rates observed at the temperature maximum could be maintained throughout the entire curve. The high rate of oxygen evolution is due to the fact the oxygen evolution and photoassembly at 28 °C is at its most efficient so it takes fewer photons and less $K_3[Fe(CN)_6]$ to get the maximum oxygen evolution. The effect of $K_3[Fe(CN)_6]$ on the temperature profile was evidence that under oxidant limiting conditions, photoassembly was

acceptor side limiting. This acceptor side limitation of photoassembly could indicate that the acceptor side limiting model of photoinhibition is the correct model that has been presented.

Preliminary kinetics experiments have been conducted in order to probe the photoassembly model proposed by Cheniae (Figure 26). By attempting to perform photoassembly using only a 1 s pre-flash followed by a long dark step to allow for dark rearrangement, initial results indicate that there is at least one dark dependent intermediate that is not shown in the original Cheniae model. The 1 s pre-flash was a repeat of work done by Kolling et al. and this experiment is significant because it is a 1 s bulk photon pulse as opposed to the train of pulses that is normally used to perform photoassembly. Because the illumination was just 1 exposure to light followed by the dark adaptation step, kinetics can truly be probed where as the pulse train does not allow for the probing of these types of kinetics.

Future Work

There still need to be more experiments conducted to fully elucidate this mechanism of photoassembly, but, through the mapping of the temperature dependence and its optimization, these experminets will much easier to perform and observe on the clark type electrode. Future kinetics experiments will be conducted in order to more completely elucidate the new model for photoassembly. pH experiments will be required to determine ligand binding sites for the manganese cluster.

To further probe the mechanism of photoinhibition, it will be necessary to study photoassembly under non-oxidant limiting conditions in order to further lend credence to the acceptor side limited mechanism for photoinhibition. These experiments will require finding a redox mediator that can be used for photoassembly; some of the most promising redox mediators

are conductive carbon nanotubes or conductive nanoparticles. This will also allow for truly probing the rate limiting step of photoassembly and will result in a much fuller understanding of photoassembly and its mechanisms.

In order to help verify the new model for photoassembly that has been proposed, kinetics simulations will need to be run. The simulations will involve writing the program and plugging in the data that have been obtained and verifying that the model is indeed feasible. Pulse experiments will also need to be designed in order to further test and verify the new model.

Reference

1. Baranov, S. V., A. M. Tyryshkin, D. Katz, G. C. Dismukes, G. M. Ananyev, and V. V. Klimov. 2004. Bicarbonate Is a *Native* Cofactor for Assembly of the Manganese Cluster of the Photosynthetic Water Oxidizing Complex. Kinetics of Reconstitution of O_2 Evolution by Photoactivation. Biochemistry 43:2070-2079.

2. Schiller, H.; Dau, H. 2000. Preparation protocols for high activity Photosystem II membrane particles of green algae and in higher plants, pH dependence of oxygen evolution and comparison of the S_2-state multiline signal by X-band EPR spectroscopy. Journal of Photochemistry and Photobiology. 55:138-144.

3. Berthold, D. A., Babcock, G. T., and Yocum, C. F. 1981. A highly resolved, oxygen-evolving photosystem II preparation from spinach thylakoid membranes: EPR and electron-transport properties. FEBS Lett. 134:231-234.

4. Kolling, D.R.J., Brown T.S., Ananyev G., Dismukes C.G. 2009. Photosynthetic Oxygen Evolution Is Not Reversed at High Oxygen Pressures: Mechanistic Consequences for the Water-Oxidizing Complex. Biochemistry. 48:1381-1389.

5. Reece, S.Y., Hamel, J.A., Sung, K., Jarvi, T.D., Esswein, A.J., Pijpers, J.J.H., Nocera, D.G. 2011. Wireless Solar Water Splitting Using Silicon-Based Semiconductors and Earth-Abundant Catalysts. Science. 334:645-648

6. Xu, B., Bhawe, Y., Davis, M.E. 2012. Low-temperature, manganese oxide-based, thermochemical water splitting cycle. Proceedings of the National Academy of Sciences of the USA. 109:9260-9264.

7. Vermaas, W. An Introduction to Photosynthesis and Its Applications. *World & I* **1998,** 158-165.

8. Blankenship, R.E. *Molecular Mechanisms of Photosynthesis;* Wiley-Blackwell: 2002

9. Liu, F., Concepcion, J.J., Jurss, J.W., Cardolaccia, T., Templeton, J.L., Meyer T.J. 2008. Mechanisms of Water Oxidation from the Blue Dimer to Photosystem II. *Inorganic Chemistry.* 47:1727–1752

10. Yaris L. News center.lbl.gov. http://newscenter.lbl.gov/press-releases/2009/03/10/turning-sunlight-into-liquid-fuels-berkeley-lab-researchers-create-a-nano-sized-photocatalyst-for-artificial-photosynthesis/.

11. Hipkins, M. F., Baker, N. R. *Photosynthesis energy transduction*; practical application series; IRL Press Limited: Eynsham, England, 1986; pg 1-7.

12. Tyystjärvi, E. 2008. Photoinhibition of Photosystem II and photodamage of the oxygen-evolving manganese cluster. Coordination Chemistry Reviews. 252:361–376.

13. Vass, I., Styring, S., Hundal, T., Koivuniemi, M., Aro, E-M., Andersson, B. 1992. Reversible and irreversible intermediates during photoinhibition of photosystem II: Stable reduced Q_A species promote chlorophyll triplet formation. Proceedings of the National Academy of Sciences of the USA. 89:1408–1412.

14. Callahan, F.E., Becker, D.W., Cheniae, G.M. 1986. Studies on the Photoactivation of the Water-Oxidizing Enzyme: II. Characterization of Weak Light Photoinhibition of PSII and Its Light-Induced Recovery. Plant Physiology. 82:261–269.

15. Eckert, H.J., Geiken, B., Bernarding, J., Napiwotzki, A., Eichler, H.J., Renger, G. 1991. Two sites of photoinhibition of the electron-transfer in oxygen evolving and Tris-treated PS-II membrane-fragments from spinach. Photosynthesis Research. 27:97–108.

16. Hakala, M., Tuominen, I., Keränen, M., Tyystjärvi, T., Tyystjärvi, E. 2005. Evidence for the role of the oxygen-evolving manganese complex in photoinhibition of Photosystem II. Biochimica et Biophysica Acta – Bioenergetics. 1706: 68–80.

17. Santabarbara, S., Cazzalini, I., Rivadossi, A., Garlaschi, F.M., Zucchelli, G. Jennings, R.C. 2002. Photoinhibition *in vivo* and *in vitro* involves weakly coupled chlorophyll-protein complexes. Photochemistry and Photobiology. 75:613–618.

18. Jung, J., Kim, H-S. 1990. The chromophores as endogenous sensitizers involved in the photogeneration of singlet oxygen in spinach thylakoids. Photochemistry and Photobiology. 52:1003–1009.

19. Keren, N., Berg, A., Van Kan, P.J.M., Levanon, H., Ohad, I. 1997. Mechanism of photosystem II photoinactivation and D1 protein degradation at low light: The role of back electron flow. Proceedings of the National Academy of Sciences of the USA. 94:1579–1584.

20. Renger, G. Oxygen evolution. *Photosynthetic Oxygen evolution;* Editor, H., Metzner; Academic Press: London, England, 1978; pg. 229-248.

21. Mirco.magnet.fsu.edu http://micro.magnet.fsu.edu/cells/plantcell.html (accessed March 6, 2013)

22. Micro.magnet.fsu.edu http://micro.magnet.fsu.edu/cells/chloroplasts/chloroplasts.html (accessed March 6, 2013)

23. Schiller, H.; Dau, H. 2000. Preparation protocols for high activity Photosystem II membrane particles of green algae and in higher plants, pH dependence of oxygen evolution and comparison of the S_2-state multiline signal by X-band EPR spectroscopy. Journal of Photochemistry and Photobiology 55:138-144.

24. Sproviero, E.M., Jose, A.G., McEvoy, J.P., Brudvig, G.W., Batista, V.S. 2008. Quantum Mechanics/Molecular Mechanics Study of the Catalytic Cycle of Water Splitting in Photosystem II. Journal of the American Chemical Society. 130:3428-3442.

25. Burnap, R.L. 2004. D1 protein processing and Mn cluster assembly in light of the emerging Photosystem II structure. Journal of Physical Chemistry. 6:4803-4809.

26. Barber, J. 2006. Photosystem II: an enzyme of global significance. Biochemical Society Transactions. 34:619-631.

27. Kolling, D.R.J., Cox, N. Ananyev, G.M., Pace, R.J., Dismukes, G.C. 2012. What Are the Oxidation States of Manganese Required To Catalyze Photosynthetic Water Oxidation? Biophysical Journal. 103:1-10.

28. Umena, Y., Kawakami, K., Shen, J-R., Kamiya, N. 2011. Crystal structure of oxygen-evolving photosystem II at a resolution of 1.9Å. Nature. 0:1-8

29. Semin, B.K., Seibert, M. 2009. A simple colorimetric determination of the manganese content in photosynthetic membranes. Photosynthesis Research. 100:45-48.

30. Serrat, F.B. 1998. 3,3□,5,5□-Tetramethylbenzidine for the Colorimetric Determination of Manganese in Water. Mikrochim. Acta. 129:77-80.

31. Kato, Y., Sun, X., Zhang, L., Sakamoto, W. 2012. Cooperative D1 Degradation in the Photosystem II Repair Mediated by Chloroplastic Proteases in Arabidopsis. Plant Physiology. 159:1428-1439.

32. Eckert, H-J., Renger, G. 1988. Temperature dependence of $P680^+$ reduction in O_2-evolving PS II membrane fragments at different redox states S_i of the water oxidizing system. Febbs Letters. 236:425-431.

33. Cheniae, G.M., Martin, J.F. 1972. Effects of Hydroxylamine on Photosystem II. Plant Physiology. 50:87-94.

34. Tamura, N., Inoue, Y., Cheniae, G.M. 1989. Photoactivation of the water-oxidizing complex in Photosystem II membranes depleted of Mn, Ca and extrinsic proteins. II. Studies of the function of Ca^{2+}. Biochimica et biophysica acta. Bioenergetics. 976:173-181.

35. Zaltsman, L., Ananyev, G.M., Bruntrager, E., Dismukes, G.C. 1997. Quantitative Kinetic Model for Photoassembly of the Photosynthetic Water Oxidase from Its Inorganic Constituents: Requirements for Manganese and Calcium in the Kinetically Resolved Steps. Biochemistry. 36:8914-8922.

36. Mulo, P., Laakso, S. Mäenpää, P., Aro, E-M. 1998. Stepwise Photoinhibition of Photosystem II. Plant Physiology. 117:483-490

Appendix A (BBY Prep)

BBY Preparation Protocol

Night before prep: obtain ~4 bunches of spinach (small, soft, smooth leaves with short stems). Remove stems and place leaves in plastic bags filled with DI water. Incubate bags at 4˚C overnight.

BBY Preparation:

-use 100 μM ε-ACA and 40 μM PMSF in all buffers throughout prep

1. Grind leaves with juice maker. Yield should be a total of 1 L. Mix with protease inhibitors while grinding.
2. Filter suspension through 8 layers of synthetic cheese cloth.
3. Place filtrate into 250 mL centrifuge tubes and spin at 4500 rpm in a JA14 for 1-2 min. at 4˚C (3000 Xg).
4. Collect supernatant and spin at 7500 rpm in a JA14 for 15 min. at 4˚C (8600 Xg).
5. Resuspend the pellet in a minimal volume of **K2** buffer (~ 50 mL) using a brush and homogenizer and then determine the [chlorophyll]: mix 995 μL 80% (v/v) acetone and 5 μL of prep in an Eppendorf tube, mix thoroughly, and spin in microfuge for 30 sec. Measure OD_{652} and OD_{750}, then calculate [chlorophyll], and dilute to 2.5 mg/mL chlorophyll.

[Chl] (mg/mL) = ((OD_{652} – OD_{750}) x optical path length (cm) x 27.8 x D.F. / 1000)

6. Place suspension in a beaker. Stir slowly (setting ~7-8) with a magnetic stirrer and add Triton X-100 (20% w/v) slowly along the walls of the beaker until reaching 20 mg Triton X-100: 1 mg Chl. The final [Chl] should be ~ 2 mg/mL. Stir for 12 min. and transfer to 42 mL centrifuge tubes. (Triton vol. = 1/5 total vol.)

   -detergent eats away at the ends of the grana

7. Spin in a JA20 at 18,000 rpm for 18 min. at 4˚C. (Note: total time in Triton X-100 should not exceed 30 min.) Decant supe: this contains mostly antenna and PSI. (40,000 Xg)
8. Resuspend pellet in **K2** buffer and place in 4, 42 mL centrifuge tubes, filling the rest with **K2**, and spin in a JA20 at 40 000 Xg for 18 min. at 4˚C.

9. Resuspend the pellets in **K3** (try not to resuspend white pellet at bottom, this is starch) and place into 2 42 mL centrifuge tubes. Spin at 18,000 rpm in a JA20 for 18 min. at 4˚C. If the supe is clear, resuspend the pellet in a minimal volume of **K3** (2.5 mg/mL), and freeze at liquid nitrogen temperature (77 K). If the supe is not clear, repeat the **K3** buffer wash.

Taken from Dismukes group lab protocol binder (DK)

Updated October, 30, 2011 (JB)

Appendix B (apo-prep)

Apo-PSII Prep. for Small Scale Photoactivation

1. Slowly thaw the BBY particles to 0 °C in the dark after removal from the liquid nitrogen
2. Measure the [Chl *a*] using the equation: [Chl *a*]= (A_{652} - A_{750}) * 27.8*200/1000
3. Concentrate BBYs to a [Chl *a*] of 5.25 mg/ml
4. Add in as many eppendorfs as necessary: 1ml CHES buffer, 200 µL 10mM $MgCl_2$, and 200 µL 5.25mg/ml BBY
5. Mix eppendorfs by inversion for 4 min, then quench the reaction by adding the BBY mixture to two eppendorfs containing 700 µL of K3 (the two tubes should have 700 µL of K3 and 700 µL of BBY mixture, giving you two tubes with 1.4 mL)
6. Centrifuge the eppendorfs at maximum speed for 60 sec
7. Decant off the supernatant and discard it in a waste container, then resolublize each pellet in 1 mL of K3 and spin for 60 sec
8. The pellets are washed in 1 mL of K3 3 more times. By the third wash the pellet will likely have gotten softer and the supernatant will need to be removed by pipette to avoid pouring out the pellet.
9. After the final wash resolublize the pellet with enough K3 to bring the [Chl] to 2.5 mg/mL

For testing the **APO-BBY activity:**

A sample is prepared with 200 µl $CaCl_2$ (stock 10mM), 100 µL of $K_4[Fe(CN)_6]$ (stock 50mM), 5 µL of APO-BBY (stock 2.5 mg/mL), and 695 µL of K3 so the final vol. is 1 mL

For **photoactivation**:

A sample is prepared with 200 µl $CaCl_2$ (stock 10mM), 100 µL of $K_4[Fe(CN)_6]$ (stock 50mM), 50 µL of $MnCl_2$ (stock 2mM), 50 µL of sodium bicarbonate (stock 20mM), 5 µL of APO-BBY (stock 2.5 mg/mL), and 595 µL of K3 so the final vol. is 1 mL

Appendix C (SDS-PAGE)

1. 50 µL of BBY sample was mixed with an equal amount of DTT and SDS and heated at 95 °C for 10 minutes.

2. The sample then had loading dye added to it and a 10 µL sample was loaded into a 4-12% precast gel

3. Electrophoreses was then performed at 200 mV for 45 min to get the desired separation.

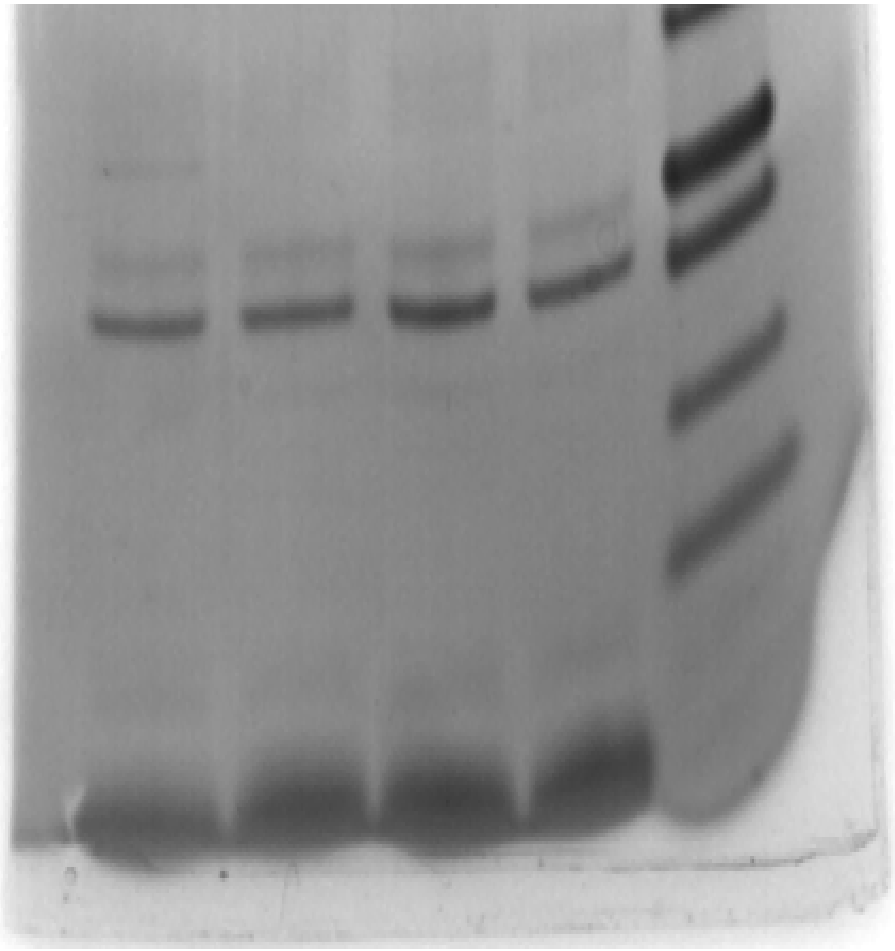

Appendix D (Mn-assay)

Table 1: Results for the spectroscopic analysis of Mn in standard solutions of Mn, BBY particles with and without a Ca-wash, and apo-BBY particles with and without a Ca-wash.

Sample	Absorbance at 450 nm	[Mn] µM
Standard 1	0.023	0.94
Standard 2	0.011	0.47
Standard 3	0.006	0.24
Standard 4	0.003	0.094
Standard 5	0.001	0.047

Table 2: Results for the Mn content of BBY particles with and without a Ca-wash, and apo-BBY particles with and without a Ca-wash.

Sample	[Mn] µM	Mn per PSII
BBY 1	50.929	6.27
BBY 2	45.921	5.65
BBY 3	51.113	6.29
BBY Ca-Washed 1	42.935	5.28
BBY Ca-Washed 2	46.541	5.72
BBY Ca-Washed 3	43.785	5.38
Apo BBY 1	1.746	1.55
Apo BBY 2	4.204	3.74
Apo BBY 3	1.263	1.12
Apo-BBY Ca-Washed 1	0.046	0.04
Apo-BBY Ca-Washed 2	0.000	0

Table 3: Results for the Chl content of BBY particles and apo-BBY particles		
Sample	[Chl *a*+*b*] µM	[PSII] µM
BBY 1	2040	8.16
BBY 2	2196	8.78
BBY 3	1859	7.44
Apo-BBY 1	273.3	1.09
Apo-BBY 2	285.2	1.14
Apo-BBY 3	284.1	1.14

Appendix E (IRB Approval)

MARSHALL UNIVERSITY
www.marshall.edu

Office of Research Integrity

April 2, 2013

James S. Board II
Chemistry Department
Marshall University

Dear Mr. Board:

This letter is in response to the submitted thesis abstract titled "Towards a Comprehensive Model of PSII OEC Photoassembly." After assessing the abstract it has been deemed not to be human subject research and therefore exempt from oversight of the Marshall University Institutional Review Board (IRB). The Code of Federal Regulations (45CFR46) has set forth the criteria utilized in making this determination. Since the information in this study does not involve human subjects as defined in the above referenced instruction it is not considered human subject research. If there are any changes to the abstract you provided then you would need to resubmit that information to the Office of Research Integrity for review and a determination.

I appreciate your willingness to submit the abstract for determination. Please feel free to contact the Office of Research Integrity if you have any questions regarding future protocols that may require IRB review.

Sincerely,

Bruce F. Day, ThD, CIP
Director
Office of Research Integrity